Petroleum potential of the Upper Jurassic Hareelv Formation, Jameson Land, East Greenland

Jørgen A. Bojesen-Koefoed, Morten Bjerager, H. Peter Nytoft, Henrik I. Petersen, Stefan Piasecki and Anders Pilgaard

The marine, mudstone-dominated Hareelv Formation (Upper Jurassic) of Jameson Land, East Greenland is a representative of the widespread Kimmeridge Clay Formation equivalents, *sensu lato*, known from the greater North Atlantic region, western Siberia and basins off eastern Canada. These deposits constitute the most important petroleum source-rock succession of the region. The present study reports petroleum geochemical data from the 233.8 m thick succession penetrated by the fully cored Blokelv-1 borehole, and includes supplementary data from outcrop samples and other boreholes in Jameson Land. The succession consists of basinal mudstone intercalated with a significant proportion of gravity-flow sandstones, both *in situ* and remobilised as injectites. The mudstones are generally rich in organic carbon with values of TOC reaching nearly 19 wt% and high pyrolysis yields reaching values of S2 up to nearly 43 kg HC/ton. Hydrogen Indices are up to 363. The data presented herein demonstrate that weathering of abundant pyritic sulfur adversely affects the petroleum potential of the kerogen in outcrop samples. The succession is thermally immature to early mature, except where intrusions have locally heated adjacent mudstones. The documentation of rich gas/oil-prone Upper Jurassic successions in Jameson Land is important for the assessment of the regional petroleum potential, including the North-East Greenland continental shelf.

Keywords: East Greenland, Upper Jurassic, petroleum source rock, generation potential, thermal maturity.

J.A.B.K., M.B., H.P.N. & S.P., *Geological Survey of Denmark and Greenland, Øster Voldgade 10, DK-1350 Copenhagen K, Denmark.* E-mail: *jbk@geus.d*k

H.I.P., *Total Exploration & Production Denmark, Amerika Plads 29, 2100 Copenhagen K, Denmark*

S.P., also *Geological Museum, Natural History Museum of Denmark, University of Copenhagen, Øster Voldgade 5-7, DK-1350 Copenhagen K, Denmark*

A.P., *Dansk Miljørådgivning A/S, Karolinevej 17, DK-4200 Slagelse, Denmark*

Oxfordian–Ryazanian marine shales form the most important petroleum source rocks of the prospective basins of the North Atlantic region. These include the basins of the greater North Sea area, the Barents Shelf, the basins west of Ireland and the Shetland Islands, the Jeanne d'Arc and Flemish Pass basins off eastern Canada as well as the basins of western Siberia, and probably also the hitherto untested basins off East and North-East Greenland. The deposits have been the subjects of numerous studies (e.g. von der Dick *et al*. 1989; Miller 1990; Chakhmakhchev *et al*. 1994; Klemme 1994; Telnæs *et al*. 1994; Fowler & McAlpine 1995; Isaksen & Ledje 2001; Ineson *et al*. 2003; Justwan & Dahl 2005; Justwan *et al*. 2005, 2006a,b; Petersen *et al*. 2010), and age-equivalent rocks crop out onshore North-East Greenland. Despite their importance for future exploration in the East and North-East Greenland offshore region, published in-depth studies of their nature and petroleum potential have hitherto been scarce, with a few notable exceptions (Requejo *et al*. 1989; Christiansen *et al*. 1992; Strogen *et al*. 2005). During the

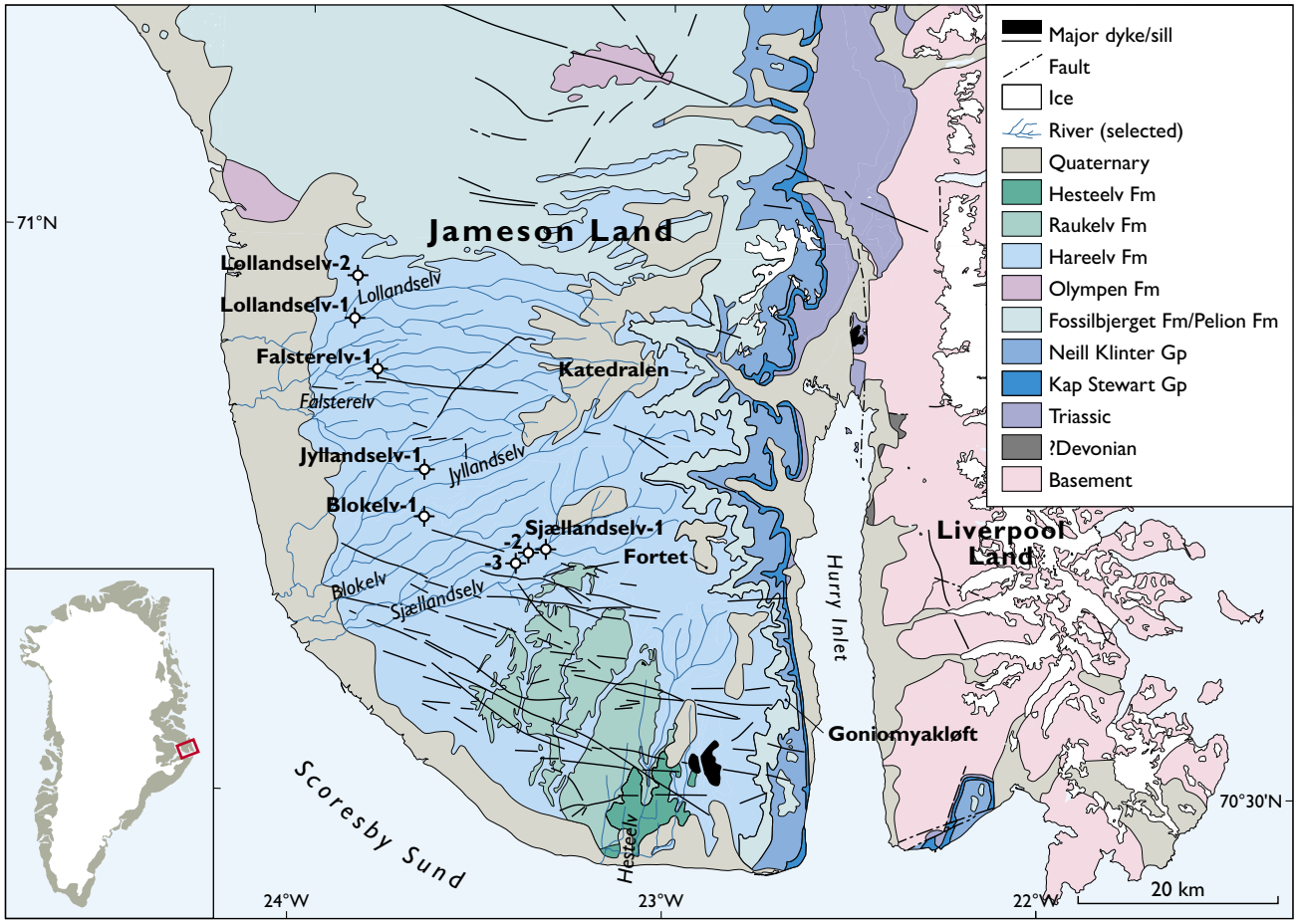

Fig. 1. Geological map of Jameson Land showing outcrop sampling areas mentioned in the text, locations of the 'old boreholes' (Lollandselv-1, -2, Falsterelv-1, Jyllandselv-1, Sjællandselv-1, -2, -3) and the Blokelv-1 borehole. Inset shows the location of southern Jameson Land in East Greenland.

period 2008–2010, the Geological Survey of Denmark and Greenland (GEUS) drilled three fully cored boreholes to depths of more than 200 m targeting the Upper Jurassic – Lower Cretaceous shale succession in East and North-East Greenland. The deposits are roughly time-equivalents of the Kimmeridge Clay Formation of the Wessex Basin, UK, and comparable core material exists from the Kimmeridge Clay Formation close to its type section in Dorset (Morgans-Bell *et al.* 2001). However, the East and North-East Greenland cores offer a unique opportunity to study nearly the full succession, which ranges in age from Oxfordian to Ryazanian, in an area remote from other studied outcrops and wells. The first of these boreholes to be drilled was Blokelv-1 in Jameson Land, which covers the succession from the Oxfordian to the Lower Volgian. The objective of this paper is to present a comprehensive overview of the petroleum potential of the Upper Jurassic – Lower Cretaceous shale succession in Jameson Land, based on new evidence from the Blokelv-1 core, while including other available data from both outcrops and earlier shallow, fully cored boreholes drilled in Jameson Land (Fig. 1). Details of the drilling, sedimentology and stratigraphy of the Blokelv-1 borehole can be found in Bjerager *et al.* (2018a, b, this volume) and Alsen *et al.* (2018, this volume).

Geological setting

The Jameson Land Basin is interpreted as a rift basin bounded by faults against Caledonian basement rocks to the west and against the uplifted basement rocks of Liverpool Land to the east (Hamann *et al.* 2005, and references therein). The nature of the northern and southern limits of the basin is unclear, although deep-seated NW–SE-trending faults on the northern part of Jameson Land

have been interpreted to have influenced the depositional patterns in the Jurassic and may mark the transition to the Traill Ø basin (Dam *et al*. 1995). The tectonic style changes north of Jameson Land towards the Wollaston Forland Basin where the structural style is dominated by westerly tilted fault blocks (Vischer 1943; Surlyk 1978). The fill of the Jameson Land Basin consists of Devonian to Cretaceous sediments with a composite thickness of up to 17 km. The basin fill is gently tilted (2–3°) towards the SW, and younger deposits are thus primarily present in southern Jameson Land. The succession includes Oxfordian–Ryazanian marine organic-rich mudstones (Christiansen *et al*. 1992, 1993), broadly age-equivalent to the widespread, rich petroleum source-rock successions of the offshore areas of Northwest Europe. Such deposits are also widespread in other areas of East and North-East Greenland, where they are referred to several lithostratigraphic units (Surlyk 2003).

In Jameson Land, this succession is referred to the Olympen, Hareelv, Raukelv and Hesteelv Formations (Fig. 2); Bjerager *et al*. (2018c, this volume) provide details of the stratigraphy and regional geology. The upper part of the Olympen Formation is represented by shallow marine deltaic sandstones with a transition downslope to bioturbated silty mudstones and gravity-flow sandstones. In the basinal settings, the formation passes up into the lower slope to basinal Hareelv Formation (*Hareelv* = Hare River; lower Oxfordian – lower Volgian) which is up to 200 m thick in the eastern part of the basin and may reach thicknesses of 300–500 m more centrally in the basin. Organic-rich marine mudstones are largely restricted to the Katedralen Member (Oxfordian–Kimmeridgian),

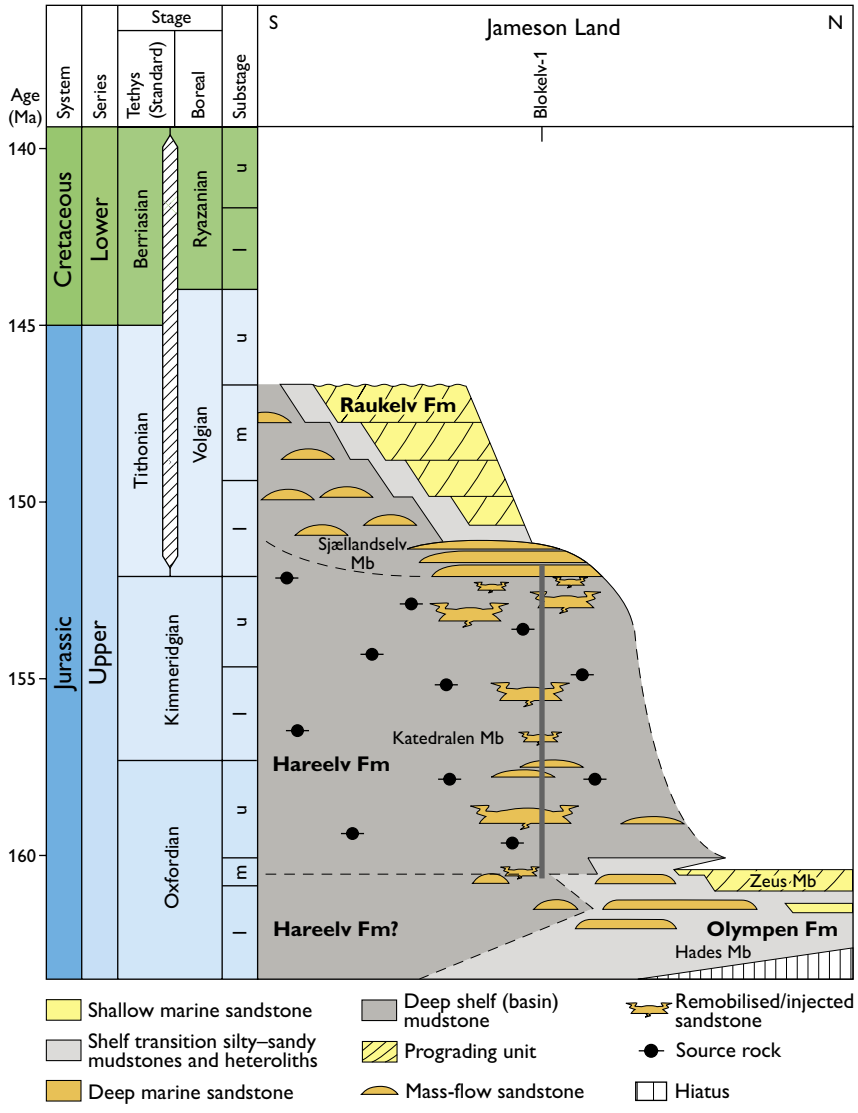

Fig. 2. Stratigraphic framework (modified from Bjerager *et al*. 2018c, this volume) showing the stratigraphic range of the cored Blokelv-1 borehole.

Table 1. Overview of cored boreholes and outcrop samples

		Core-ID	Drilled	Latitude	Longitude	Depth (m)	Age	Samples analysed
Core	Blokelv-1	511101	2008	70°45.305´	23°40.430´	233.8	M. Oxfordian – L. Volgian	139
	Sjællandselv-1	303114	1983	70°42.0'	23°25.0'	30.53	U. Kimmeridgian – L. Volgian	40
	Sjællandselv-2	303115	1983	70°42.0'	23°25.0'	40.28	U. Kimmeridgian – L. Volgian	21
	Sjællandselv-3	303116	1983	70°42.0'	23°25.0'	44.62	U. Kimmeridgian – L. Volgian	43
	Lollandselv-1	303139	1993	70°55.63'	23°50.53'	101.2	L. Oxfordian	30
	Lollandselv-2	303140	1993	70°58.00'	23°49.02'	85.5	L. – M. Oxfordian	38
	Falsterelv-1	303141	1993	70°52.91'	23°47.94'	101.2	L. – M. Oxfordian	58
	Jyllandselv-1	303142	1993	70°47.37'	23°39.13'	73.4	U. Oxfordian	83
	Total							452
Outcrop	Blokelv area	n.a.	n.a.	n.a.	n.a.	n.a.	U. Oxfordian – Kimmeridgian	3
	Falsterelv area	n.a.	n.a.	n.a.	n.a.	n.a.	U. Oxfordian – Kimmeridgian	18
	Fortet area	n.a.	n.a.	n.a.	n.a.	n.a.	Kimmeridgian–Volgian	43
	Gonyomyakløft area	n.a.	n.a.	n.a.	n.a.	n.a.	Oxfordian	3
	Jyllandselv area	n.a.	n.a.	n.a.	n.a.	n.a.	Oxfordian–Kimmeridgian	11
	Katedralen area	n.a.	n.a.	n.a.	n.a.	n.a.	Oxfordian	26
	Lollandselv area	n.a.	n.a.	n.a.	n.a.	n.a.	Oxfordian	12
	Unspecified area	n.a.	n.a.	n.a.	n.a.	n.a.	n.a.	4
	Hesteelv area (Hesteelv Fm)	n.a.	n.a.	n.a.	n.a.	n.a.	Ryazanian	8
	Total							128

whereas the overlying Sjællandselv Member is dominated by coarser clastic facies; the Salix Dal Member, which overlies the Sjællandselv Member, is dominated by silty mudstones. Deposition of the Katedralen Member mudstones took place in a deep-water marine setting and was interrupted by frequent deposition of gravity-flow sandstones, commonly remobilised post-depositionally as injectites (Surlyk & Noe-Nygaard 2001). The Raukelv Formation, which succeeds the Hareelv Formation, represents rapid coastal progradation of coarse clastic deposits into the deep basinal areas and is capped by a prominent erosional unconformity. The overlying Hesteelv Formation, exposed near the southern coast of Jameson Land, fills a *c*. 10 km wide, U-shaped channel with a southwards plunging axis. Black mudstones of the Crinoid Bjerg Member occupy the deepest part of the channel (Surlyk *et al*. 1973; Surlyk 1973). These deposits accumulated during regional drowning in the Ryazanian. The Crinoid Member of the Hesteelv Formation is thus age-equivalent to the more organic-rich intervals of the North Sea source-rock successions (Ineson *et al*. 2003).

Samples and methods

Samples used for the present study include material from the fully cored Blokelv-1 borehole, which was drilled in 2008, as well as samples from shallow fully cored boreholes drilled in 1983 and 1993, and samples collected from outcrops in Jameson Land over several decades for a variety of purposes (Fig. 1, Table 1). The stratigraphic range covered by all boreholes and their mutual stratigraphic relationships are shown in Fig. 3, which also provides a general indication of the stratigraphic intervals covered by outcrop samples included in this study. Not all outcrop samples have been dated, but a general indication of the age of samples collected from the various sampling areas is given in Table 1. Outcrop samples represent the Hareelv Formation (predominantly the Katedralen Member with a few samples from the Salix Dal Member) and the Hesteelv Formation.

For most samples, total carbon (TC, wt%), total organic carbon (TOC, wt%) and total sulfur (TS, wt%) were determined by combustion in a LECO CS-200 induction furnace. TOC was determined after elimination of carbonate-bonded carbon by prolonged HCl treatment. Petroleum potential was determined by Rock-Eval-type pyrolysis using a Source Rock Analyzer (SRA) instrument, manufactured by Humble Instruments and Services (presently Weatherford), and calibrated against the IFP160000 standard, running a blank and an in-house control standard for every 10 analyses. For some older samples, these parameters were determined using similar methods and comparable instruments such as the Rock-Eval 2 or Rock-Eval 6. Based on the experience at the GEUS laboratory, analyses of samples from the same successions carried out over a period of more than 25 years show very good agreement, despite differences in

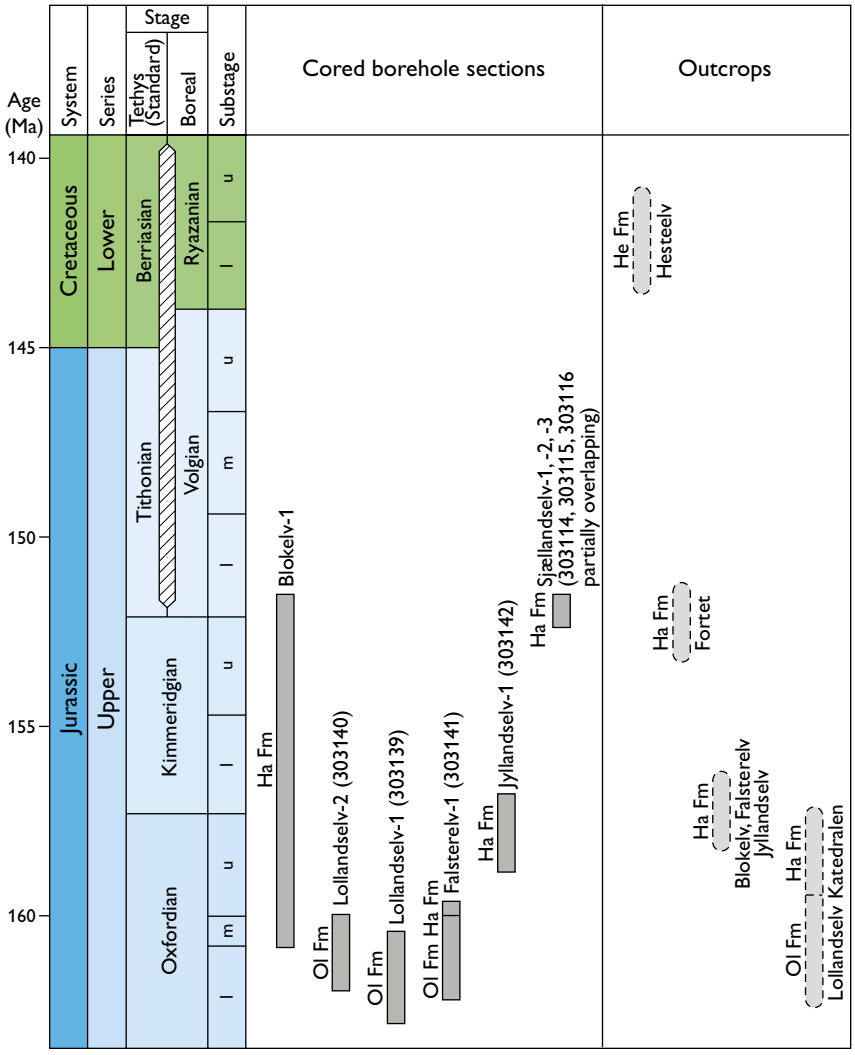

Fig. 3. Stratigraphic relationships and intervals sampled by cores and outcrops. **Ha Fm**: Hareelv Formation. **He Fm**: Hesteelv Formation. **Ol Fm**: Olympen Formation. The Greenland Geological Survey (GGU) registration number is indicated for the older suite of boreholes.

instrumentation used for analysis, provided similar calibration standards are used. Note that data published by Requejo *et al*. (1989) have been omitted here since they seem to include a calibration error with respect to T_{max}.

Particulate blocks for reflected light microscopy were prepared according to international standards (Taylor *et al*. 1998). Vitrinite reflectance (R_o) measurements (random) were made using monochromatic light (546 nm) after calibration with standards of 0.515 $\%R_o$ and 0.92 $\%R_o$. R_o for all samples was calculated from a population of vitrinite reflectance recordings selected from the measured R_o histogram. A number of samples were also qualitatively inspected in reflected white light and fluorescence-inducing blue light using a Zeiss microscope.

Solvent extraction of powdered samples (<250 μm) was carried out with methanol/dichloromethane 7:93 vol./vol. as solvent using a Soxtec equipment. Asphaltenes were precipitated with a 40-fold excess of n-pentane. Maltene fractions were separated into saturated, aromatic and NSO fractions by medium-pressure liquid chromatography (MPLC) following a procedure inspired by Radke *et al*. (1980).

Gas chromatography of saturated extract fractions was carried out using a Shimadzu GC-2010 instrument with splitless injection and a ZB-1 capillary column (25 m × 0.25 mm inner diameter, film thickness 0.10 μm). The temperature programme was 5°C/min. from 80° to 300°C, followed by 15 min. at 300°C.

Gas chromatography – mass spectrometry was carried out using an Agilent 6890N gas chromatograph connected to a Waters (Micromass) Quattro Micro GC tandem quadropole mass spectrometer. A Phenomenex ZB-5 column (30 m × 0.25 mm inner diameter, film thickness 0.10 μm) was used. The injection temperature

Fig. 4. Air photo (helicopter) of the central part of Jameson Land, viewed towards the east, showing the characteristic plateau-like landscape featuring flat-topped hills formed by the Hareelv Formation. The recessive nature of the Hareelv Formation serves to make good outcrops relatively scarce. The snow-clad mountains of Liverpool Land are visible in the distance.

was 70°C (2 min. hold). The temperature programme was 30°C/min. from 70° to 100°C and 4°C/min. from 100° to 308°C followed by 8 min. at 308°C. Argon was used as the collision gas in MS-MS runs. The saturated hydrocarbons were analysed by GC–MS in SIM-mode and by GC–MS–MS using relevant parent–daughter transitions for C_{26-30} steranes and C_{27-35} hopanes. Four separate GC–MS and GC–MS–MS methods were applied to optimise data quality. Samples were dissolved in isooctane (3 mg / ml). For a number of samples, 'vintage' biological marker data exist, but these have been omitted in order to ensure that data can be compared. Hence only biological marker data produced according to the above protocol, or similar, have been included.

Results

Outcrop samples

The Hareelv Formation is commonly poorly exposed (Fig. 4), but outcrops were sampled at a number of different locations, several situated close to borehole drill sites (Fig. 1, Table 1); samples were primarily collected from the older, Oxfordian–Kimmeridgian, parts of the succession. In general, the samples are rich in organic carbon, showing average TOC values from about 2 wt% to well over 8 wt% (Table 2). Total sulfur data are only available from the Fortet area, where the deposits show values in the range 0.3 to 3.1 wt% total sulfur (TS). The petroleum potential as indicated by the pyrolysis S2-peak

Table 2. Summary of petroleum potential data for outcrop samples, all data

		Blokelv area	Falsterelv area	Fortet area	Goniomyakløft area	Jyllandselv area	Katedralen area	Lollandselv area	Unspecified areas	Hesteelv area (Hesteelv Fm)
No. (samples)		3	18	43	3	11	26	12	4	8
TOC	Min	4.07	2.35	0.60	5.38	3.31	2.36	2.14	1.44	1.25
	Max	5.01	7.85	8.79	11.1	10.97	11.50	7.45	3.19	2.32
	Mean	4.57	4.27	4.26	8.17	7.19	7.30	4.54	2.09	1.96
T_{max}	Min	429	422	310	420	419	421	423	432	427
	Max	432	433	609	423	430	441	450	434	436
	Mean	431	427	436	421	424	429	434	433	430
S1	Min	0.61	0.02	0.00	0.14	0.16	0.02	0.01	0.02	0.05
	Max	0.64	0.30	2.33	0.75	0.46	1.62	0.04	0.07	0.22
	Mean	0.63	0.09	0.49	0.47	0.35	0.42	0.03	0.04	0.14
S2	Min	8.04	0.76	0.03	1.78	3.33	0.50	0.40	0.34	0.66
	Max	9.01	8.20	13.94	17.35	17.84	18.25	1.65	0.81	4.94
	Mean	8.58	3.22	3.57	11.49	11.27	4.80	0.99	0.58	2.46
HI	Min	173	28	2	33	76	15	13	18	53
	Max	198	180	234	191	231	171	43	36	225
	Mean	189	75	88	127	150	59	24	28	120
PI	Min	0.07	0.02	0.00	0.03	0.02	0.03	0.01	0.04	0.04
	Max	0.07	0.05	0.53	0.07	0.06	0.27	0.05	0.08	0.07
	Mean	0.07	0.03	0.15	0.05	0.04	0.07	0.03	0.06	0.06

shows wide variation with average values ranging from less than 1 kg/ton to nearly 12 kg/ton, giving average Hydrogen Index (HI) values in the range from 24 to 189 (Fig. 5, Table 2), with only a few individual samples exceeding 200. T_{max} and the Production Index (PI) consistently indicate pre-oil window maturity, except for a few samples from the Fortet and Katedralen outcrops that have been locally heated by intrusions, showing deviating data due to elevated maturity and oil staining (Fig. 5, Table 2). An attempt to establish the amount of non-reactive carbon and the average Hydrogen Index of the reactive fraction by cross-plotting S2 versus TOC (Dahl *et al*. 2004) using linear axes was unsuccessful since wide scatter precluded the construction of reliable trendlines. Systematic palynofacies data are not available, but from the study of slides for palynological dating it is known that the deposits are often very rich in woody terrestrial organic matter. In summary, despite high levels of TOC, outcrop samples in general show rather poor petroleum potential. The majority of the samples may be classified as primarily gas-prone, containing predominantly Type III kerogen, or even as non-source deposits containing predominantly inert kerogen. A few samples show HI values between 200 and 300 and may be classified as gas/oil-prone.

The Hesteelv Formation, stratigraphically overlying the Hareelv Formation and age-equivalent to the more organic-rich upper interval of the North Sea source-rock succession, is represented by a total of eight samples (Table 1). The organic carbon content is close to 2 wt%, S2 ranges from 2 to 5 kg/ton, giving Hydrogen Index values in the range 118–225 with an average of 149. All samples are thermally immature with T_{max} close to 430°C and PI close to 0.05 (Fig 5, Table 2).

'Old boreholes'

The Sjællandselv-1, -2, -3, Lollandselv-1, -2, Falsterelv-1 and Jyllandselv-1 fully cored boreholes resulted from drilling campaigns in the 1980s and 1990s and predate the drilling of the Blokelv-1 borehole in 2008; they are referred to here as 'old boreholes'. Detailed correlation of these cored sections can be found in Bjerager *et al*. 2018c, this volume.

Lollandselv-1 (core 303139), Lollandselv-2 (core 303140), Falsterelv-1 (core 303141). The three boreholes represent the lower to lowermost upper Oxfordian succession, mainly referred to the Olympen Formation but with the transition into the Hareelv Formation recorded in the top part of the Fasterelv-1 borehole (Fig. 3, Table 1); in combination, they provide a fairly complete representation of this interval. The succession is dominated by sandy deposits with subordinate mudstones that are typically silty, poorly laminated or structureless. In general, the samples collected from the cores are rich in organic carbon, showing average values between 3.8 wt% and 4.8 wt% (Table 3). The average petroleum potential, as indicated by S2, varies from 1.8 kg/ton to 4.8 kg/ton, with Hydrogen Index (HI) values ranging from 48 to 92 (Fig. 6, Table 3). T_{max} and the Production Index (PI) values indicate pre-oil window maturity.

Jyllandselv-1 (core 303142). This borehole penetrated the uppermost upper Oxfordian – lower Kimmeridgian part of the succession (Fig. 3, Table 1). The succession is dominated by mudstones, parts of which are laminated, with subordinate sandstones. The samples are rich in organic carbon with an average of 7.6 wt% (Table 3). The petroleum potential, as indicated by S2, averages 15.6 kg/ton with an average HI value of 196 (Fig. 6, Table 3). T_{max} and the Production Index (PI) generally indicate pre-oil

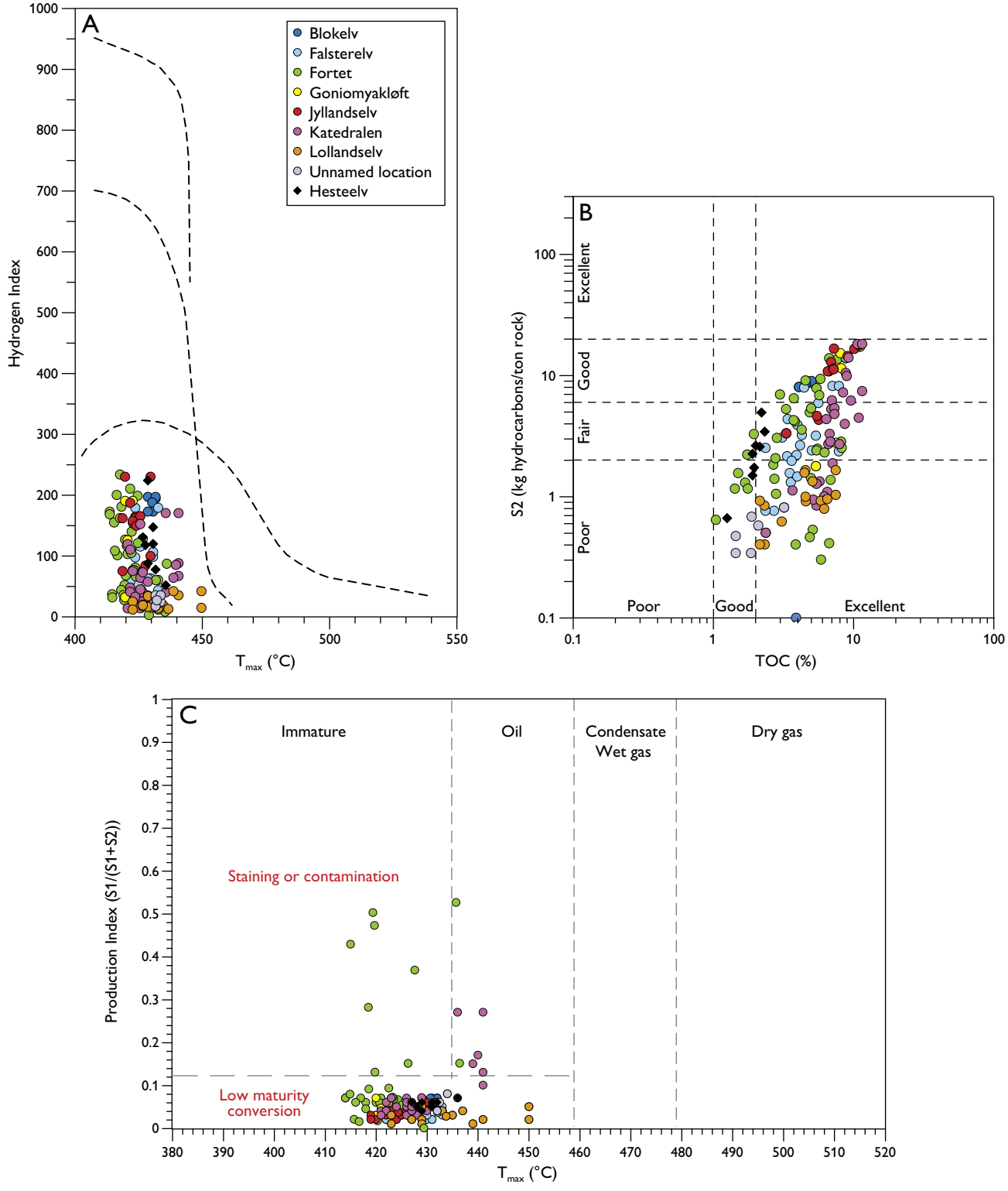

Fig. 5. Organic geochemical screening data for outcrop samples. **A**: T_{max} vs. Hydrogen Index. **B**: TOC versus S2. **C**: T_{max} vs. Production Index.

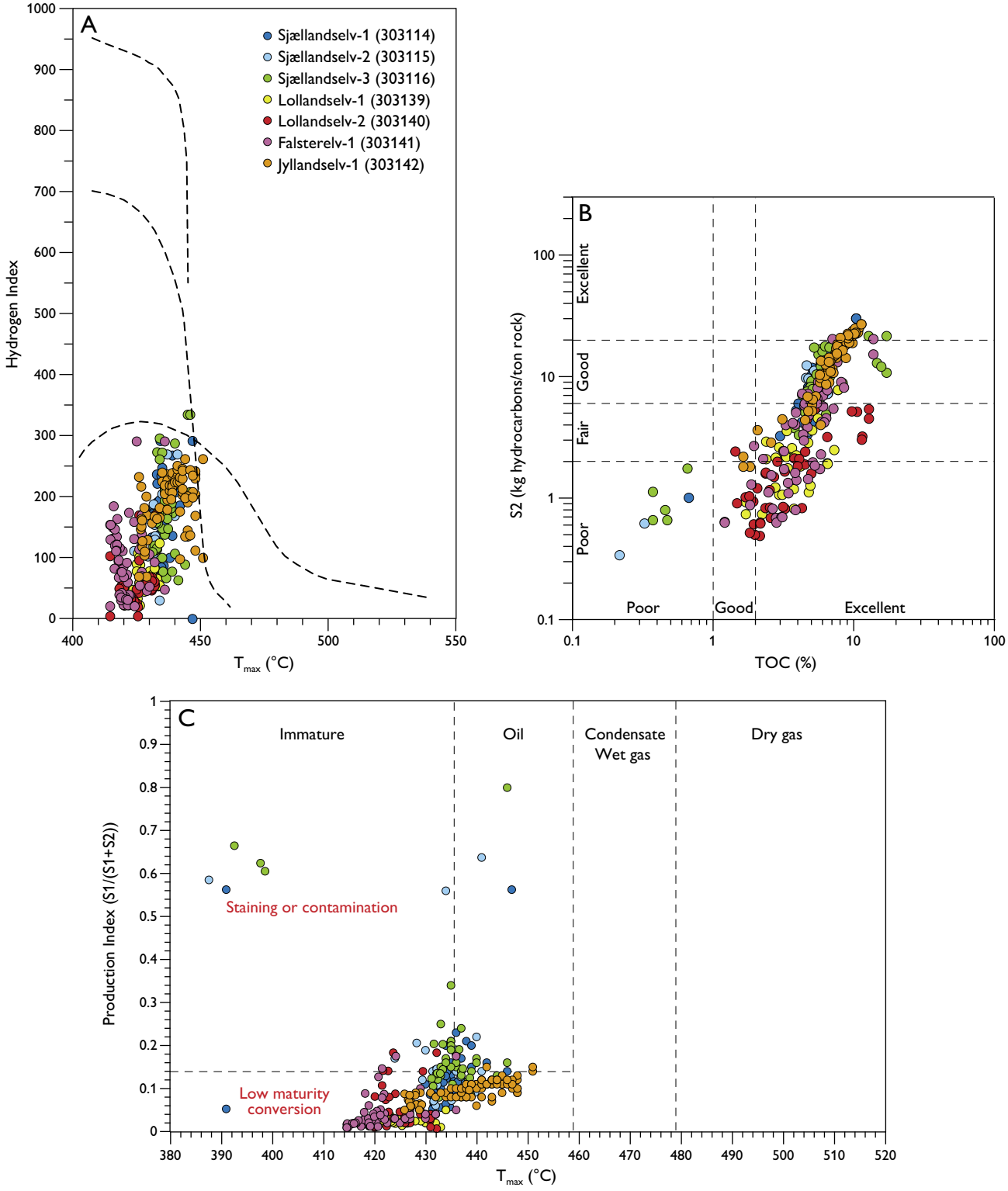

Fig. 6. Organic geochemical screening data for 'old borehole' samples. **A**: T_{max} vs. Hydrogen Index. **B**: TOC vs. S2. **C**: T_{max} vs. Production Index.

Table 3. Summary of petroleum potential data for borehole samples, all data

		Blokelv-1 borehole 511101	Sjællandselv-1 borehole 303114	Sjællandselv-2 borehole 303115	Sjællandselv-3 borehole 303116	Lollandselv-1 borehole 303139	Lollandselv-2 borehole 303140	Falsterelv-1 borehole 303141	Jyllandselv-1 borehole 303142
No. (samples)		139	40	21	43	28	38	58	83
TOC	Min	0.06	0.32	0.07	0.37	1.70	0.69	1.20	1.63
	Max	18.97	10.38	6.56	17.09	7.71	12.80	13.77	11.30
	Mean	5.94	5.58	4.71	6.02	3.89	3.98	4.78	7.56
T_{max}	Min	305	391	364	363	420	415	415	426
	Max	473	447	441	446	434	432	436	451
	Mean	430	434	428	432	426	425	421	439
S1	Min	0.00	0.02	0.48	0.52	0.01	0.00	0.02	0.28
	Max	3.43	3.29	2.62	4.55	0.23	0.40	0.55	3.13
	Mean	1.31	1.32	1.43	1.86	0.06	0.07	0.14	1.68
S2	Min	0.00	0.00	0.34	0.66	0.74	0.03	0.63	1.82
	Max	42.91	30.29	14.14	21.72	7.81	5.43	20.51	27.15
	Mean	14.76	10.11	7.91	9.28	2.26	1.84	4.84	15.55
HI	Min	3	0	30	53	22	4	21	69
	Max	363	292	270	335	124	170	291	262
	Mean	218	169	163	166	59	48	92	196
PI	Min	0.00	0.05	0.06	0.08	0.01	0.00	0.01	0.05
	Max	0.70	0.56	0.64	0.80	0.05	0.18	0.18	0.15
	Mean	0.13	0.13	0.21	0.20	0.03	0.05	0.04	0.10

window maturity, although the maturity level seems significantly higher than that recorded in the Lollandselv-1, Lollandselv-2 and Falsterelv-1 successions.

Sjællandselv-1 (core 303114), Sjællandselv-2 (core 303115), Sjællandselv-3 (core 303116). These three boreholes were drilled close together and overlap stratigraphically, together covering the upper Kimmeridgian – lowermost Volgian part of the Hareelv Formation (Katedralen Member; Fig. 3, Table 1). The upper part of the Sjællandselv-3 core overlaps with the lower portion of the Sjællandselv-2 core; the uppermost level of the latter ties with the lower Sjællandselv-1 core (see Bjerager *et al.* 2018a, this volume). The succession comprises intercalated sandy deposits and mudrocks that range from laminated to more or less structureless. In general, the mudstone samples collected from the cores are rich in organic carbon, showing average values between 4.7 wt% and 6.0 wt% (Table 3). The average petroleum potential varies from 7.9 kg/ton to 10.1 kg/ton, giving HI values in the range from 163 to 169 (Fig. 6, Table 3). On average, both T_{max} and the Production Index (PI) indicate pre-oil window maturity, but the average values mask widely varying values of both T_{max} and PI (Fig. 6).

Only the Sjællandselv-1 and Jyllandselv-1 sample sets offer the possibility to establish the amount of non-reactive carbon and the average hydrogen index of the reactive fraction by cross-plotting TOC versus S2 (Dahl *et al.* 2004) using linear axes. Datasets from other cores show too wide scatter to allow the construction of reliable trend-lines. Using only samples showing S2 > 2 kg/ton and PI < 0.12 in order to avoid non-source samples, the Jyllandselv-1 core yields an average TOC of 7.7 wt%, of which 2.6 wt% will be inert and an average Hydrogen Index for the reactive kerogen of 314 (i.e. based on an average TOC of 5.1 wt%). The Sjællandselv-1 core yields an average TOC, of 6.9 wt%, of which 3.3 wt% will be inert, and an average Hydrogen Index for the reactive kerogen of 241 (i.e. based on an average TOC of 3.6 wt%; Fig. 7). Neither systematic palynofacies data nor organic petrographic data are available, but from the study of slides for palynological dating, it is known that the deposits are often very rich in woody terrestrial organic matter.

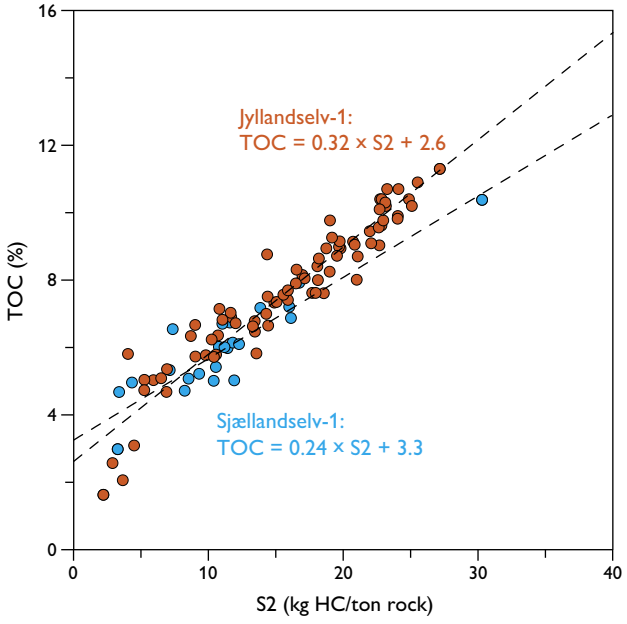

Fig. 7. Linear plot of S2 vs. TOC for samples from the Sjællandselv-1 and the Jyllandselv-1 cores; only samples showing S2 > 2 kg/ton and PI < 0.12 are used. The slope of the regression line represents the average Hydrogen Index of the reactive fraction of the kerogen. The intercept with the TOC-axis represents the average proportion of non-reactive organic carbon present (see text for discussion).

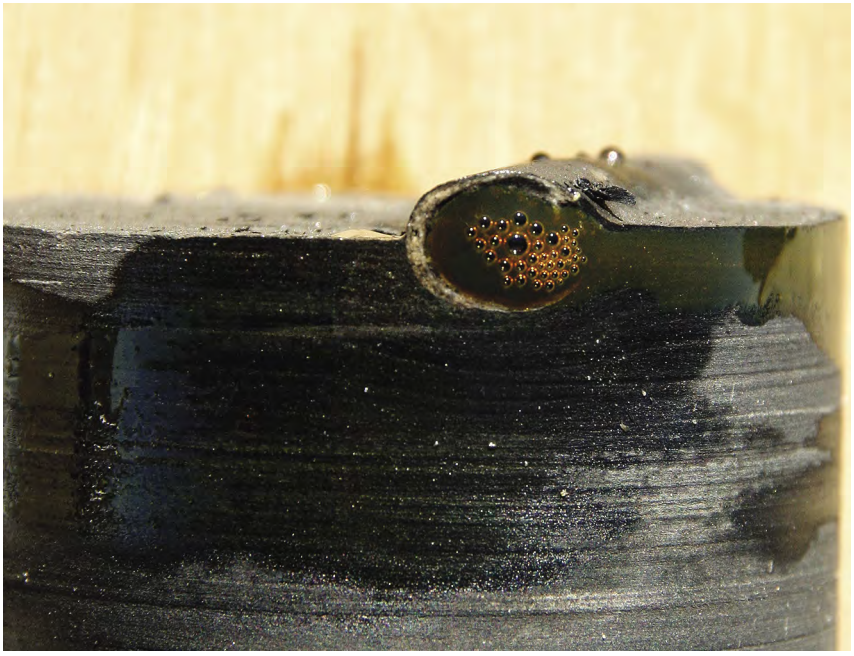

Fig. 8. Crude oil bleeding from a belemnite cut by the Blokelv-1 core (105.18 m depth). Belemnite is *c*. 16 mm in diameter (parallel to lamination).

Blokelv-1 borehole

The fully cored Blokelv-1 borehole penetrated 233.8 metres of middle Oxfordian to lower Volgian deposits (Fig. 3, Table 1), consisting of *c*. 55% mudrocks, with the remainder being gravity-flow sandstones and sandstone injectites, plus four thin basaltic intrusions up to 2 m in thickness (Bjerager *et al*. 2018b, this volume; Larsen 2018, this volume). The Blokelv-1 core covers the entire Kimmeridgian succession, which seems to be without major hiati (Alsen & Piasecki 2018, this volume), and thus represents an important portion of the Upper Jurassic that is otherwise left more or less untested by outcrop

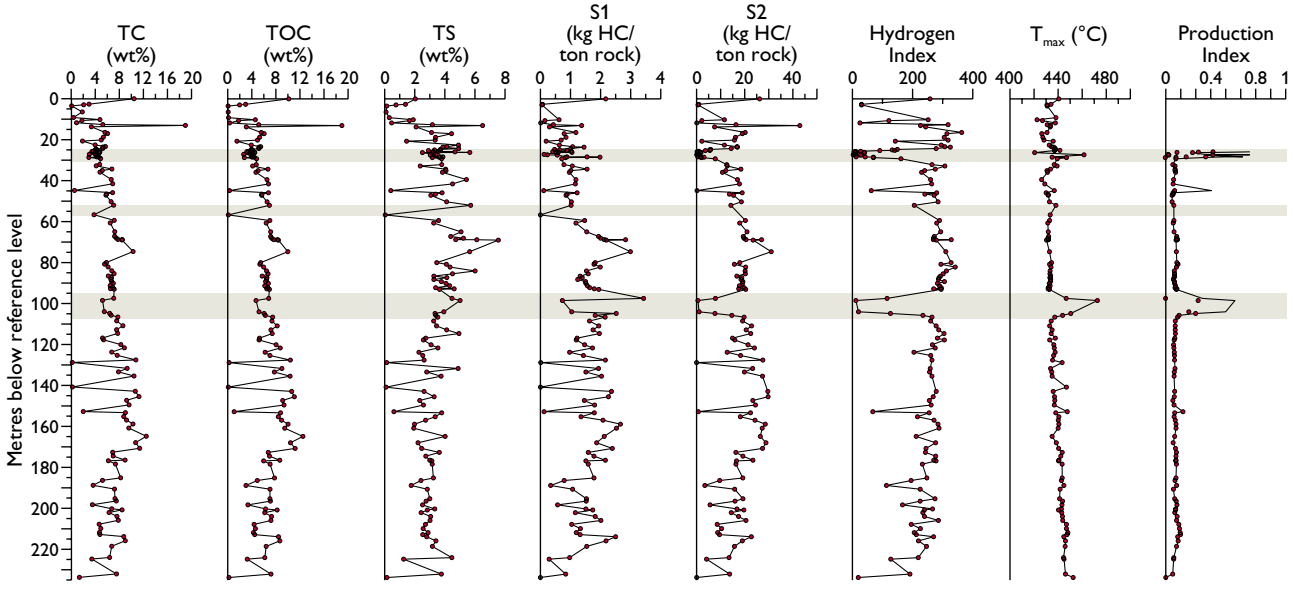

Fig. 9. Blokelv-1 core, organic geochemical screening data vs. depth. From left to right: **TC**: total carbon. **TOC**: total organic carbon. **TS**: total sulfur. S1, S2, Hydrogen Index, T_{max}, Production Index. Shading indicates approximate intervals affected by magmatic intrusions (see text for discussion).

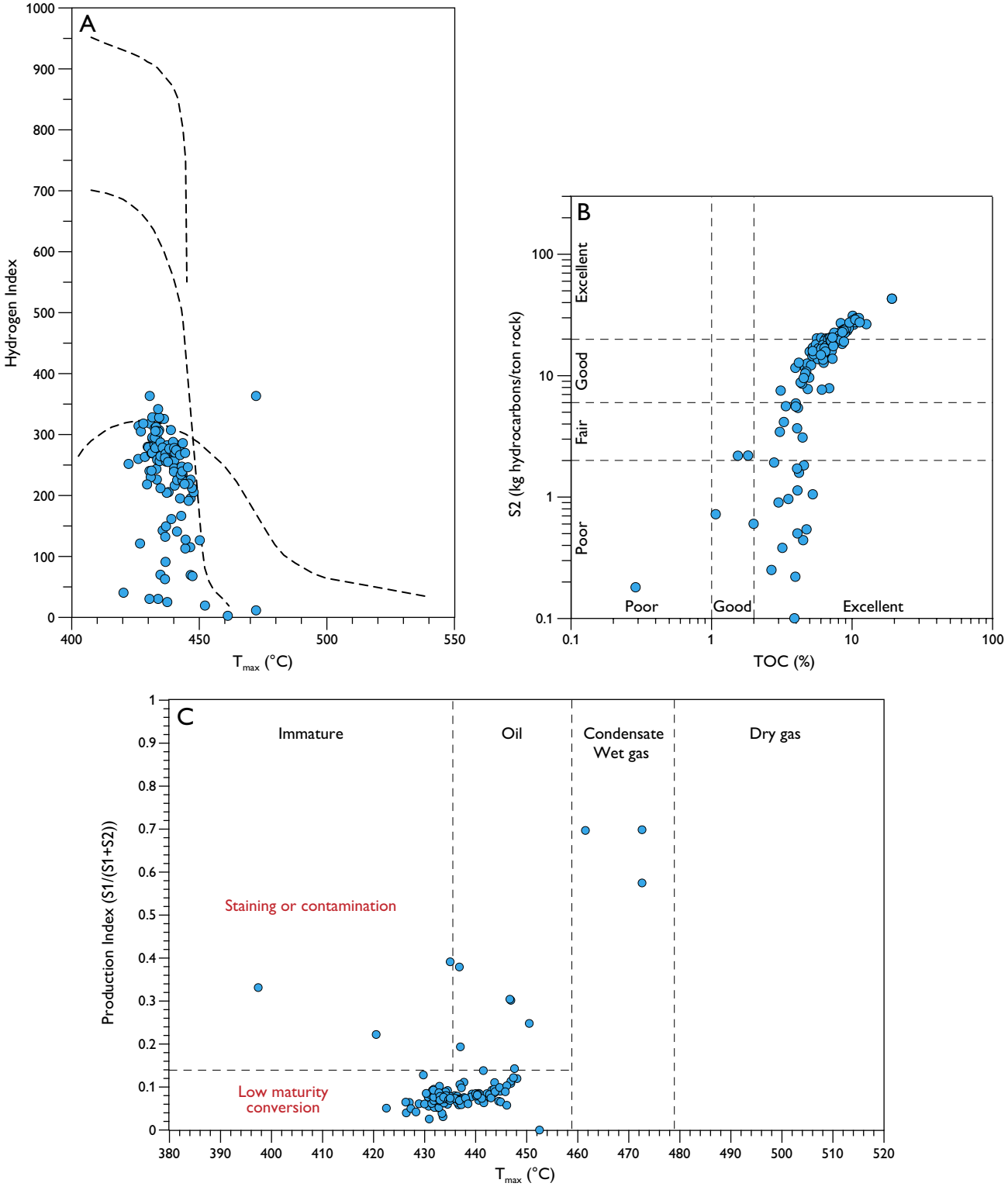

Fig. 10. Blokelv-1 core, organic geochemical screening data. **A**: T_{max} vs. Hydrogen Index. **B**: TOC vs. S2. **C**: T_{max} vs. Production Index.

sampling and borehole drilling, including the prominent Kimmeridgian sea-level highstand succession known from both the Viking Graben and East Greenland (Sneider *et al*. 1995; Surlyk 2003). A total of 139 samples were analysed for petroleum potential (Table 1). Basaltic intrusions, at *c*. 102 m, 55 m, 28 m and 7 m (Larsen 2018, this volume) resulted in the petroleum potential being more or less exhausted in a number of samples (Table 3), and petroleum generation in close proximity to the sills was also observed. At 55.4 m, oil stains were present in a carbonate-lined fracture in the intrusion itself, and liquid oil was seen flowing from the phragmocone of a belemnite at 105.25m (Fig. 8). In order to assess the overall petroleum potential of the succession, samples affected by heating from intrusions should be excluded, since intrusions are local phenomena; the following is thus based on a subset of the data (Table 5) after all samples showing S2 < 2 and PI > 0.12 were excluded.

The level of TOC is highly variable, reaching values exceeding 18 wt%, with an average TOC of nearly 7 wt% (Table 3). An irregular, but generally increasing trend in TOC extends from TD to *c*. 170 m, followed by a gradual decreasing trend that extends to the uppermost parts of the borehole (Fig. 9). The TS content shows a very irregular depth trend with initial values of 2–3 wt% from TD to *c*. 120 m, at which point a steep increase begins, culminating at *c*. 8 wt% close to 70 m, from where an irregular decreasing trend is observed, falling to values close to 1 wt% near 10 m depth. The petroleum potential as represented by S2 is strongly variable, reaching values close to 43 kg/ton, with an average S2 of nearly 18 kg/ton (Table 5). Ignoring the effects of the intrusions mentioned above, the average Hydrogen Index is fairly stable at close to 300 – slightly higher from *c*. 90 m to 10 m and slightly lower in the interval from TD to *c*. 120 m. The effects of the intrusions are clearly seen in the HI, T_{max} and PI values (Figs 9, 10C). Excluding samples affected by heating by intrusions and non-source rock samples, the succession is seen to contain primarily oil-prone type II or mixed oil- and gas-prone type II/III kerogen, with an average HI of 328 for the active kerogen and an average inert organic carbon content of only 0.95% (Fig. 11).

The thermal maturity of the succession is close to the oil window and the increasing trend in PI points to incipient generation, despite PI in absolute terms remains low (<0.12). The thermal maturity indicators consistently show an increasing trend with depth (Fig. 12A, Table 6), with the start of the oil-generative window being found somewhere between 100 m and 160 m, indicating that considerable uplift has occurred.

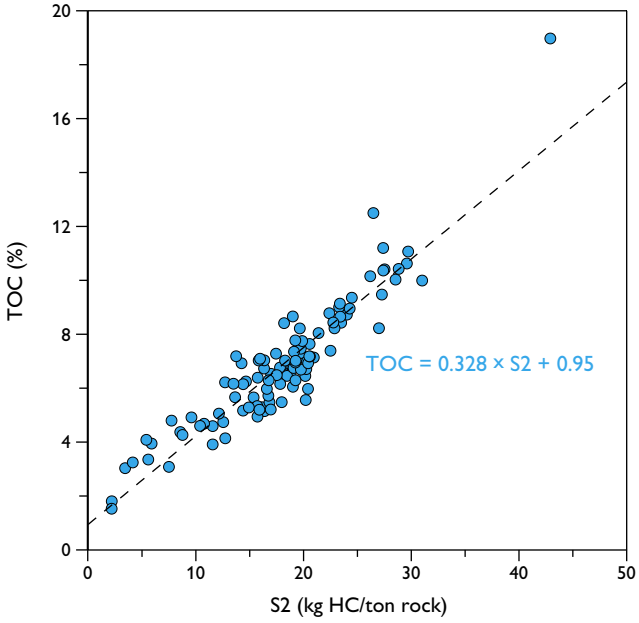

Fig. 11. Blokelv-1 core. Linear plot of S2 vs. TOC; selected data only, S2 > 2 kg/ton and PI < 0.12. The slope of the regression line represents the Hydrogen Index of the reactive fraction of the kerogen. The intercept with the TOC-axis represents the average proportion of non-reactive organic carbon present (see text for discussion).

The magmatic intrusions have had a major impact on the thermal maturity of the sedimentary rocks immediately adjacent to them, but the effects are local, restricted to an aureole around the intrusions amounting to only three to five times their thickness. An example of this is shown in Fig. 13, where the changes in Hydrogen Index (HI) and Production Index (PI) as well as in organic petrography are illustrated. Both above and below the intrusion, the HI decreases steadily approaching the intrusion as the petroleum potential is realised. The PI shows a parallel increase due to petroleum generation, but close to the intrusion, the PI shows a rapid decrease due to thermal destruction of the petroleum and generation of gaseous components that tend to escape. Under the microscope, the changes are manifest in gradually decreasing fluorescence and, closest to the intrusion, generation of pyrobitumen, coke and natural chars.

A number of different parameters, in addition to the screening data, show a gradual change with depth, with a marked shift in the trends at *c*. 90 m (Fig. 12B, Table 6). The pristane/phytane ratio shows a steady decrease from *c*. 6 at TD to values between 1 and 3 in the upper 90 m of the succession. The isohopane ratio (Nytoft 2011) decreases from more than 0.12 at TD to an average of

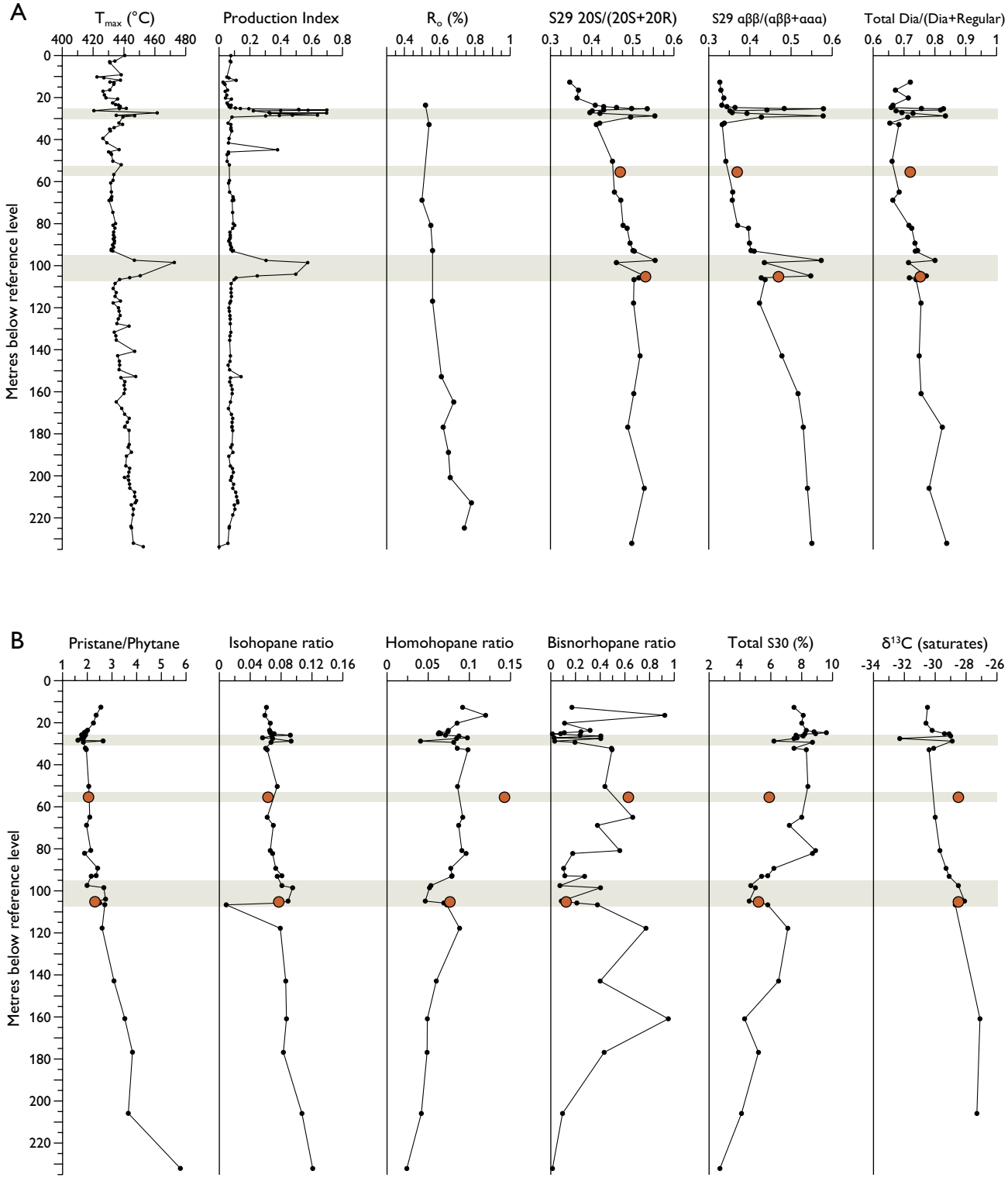

Fig. 12. **A**: Blokelv-1 core, thermal maturity indicators vs. depth. From left to right: **T_{max}** (from Rock-Eval type screening). **Production Index** (from Rock-Eval type screening). **R_o (%)**: vitrinite reflectance. **S29 20S/(20S + 20R)**: regular C_{29} sterane ααα20S/(ααα20S+ααα20R) isomer ratio. **S29 αββ/(αββ+ααα)**: regular C_{29} sterane αββ/(αββ+ααα) isomer ratio. **Total Dia/(Dia + Regular)**: sum $C_{27–29}$ diasteranes/(sum $C_{27–29}$ diasteranes + sum $C_{27–29}$ regular steranes). Red symbols indicate oil sample (stain) data. Shading indicates approximate intervals affected by magmatic intrusions (see text for discussion). **B**: Blokelv-1 core, facies indicators versus depth. From left to right: **Pristane/phytane** ratio. **Isohopane ratio** (Nytoft 2011). **Homohopane ratio**: H35/(sum H31–35). **Bisnorhopane ratio**: H28/H30. **Total S30 (%)**: percentage of C_{30} steranes relative to total $C_{27–30}$ steranes. **$\delta^{13}C$ (saturates)**: stable carbon isotope $\delta^{13}C$ of saturated extract fractions. Red symbols indicate oil sample (stain) data. Shading indicates approximate intervals affected by magmatic intrusions (see text for discussion).

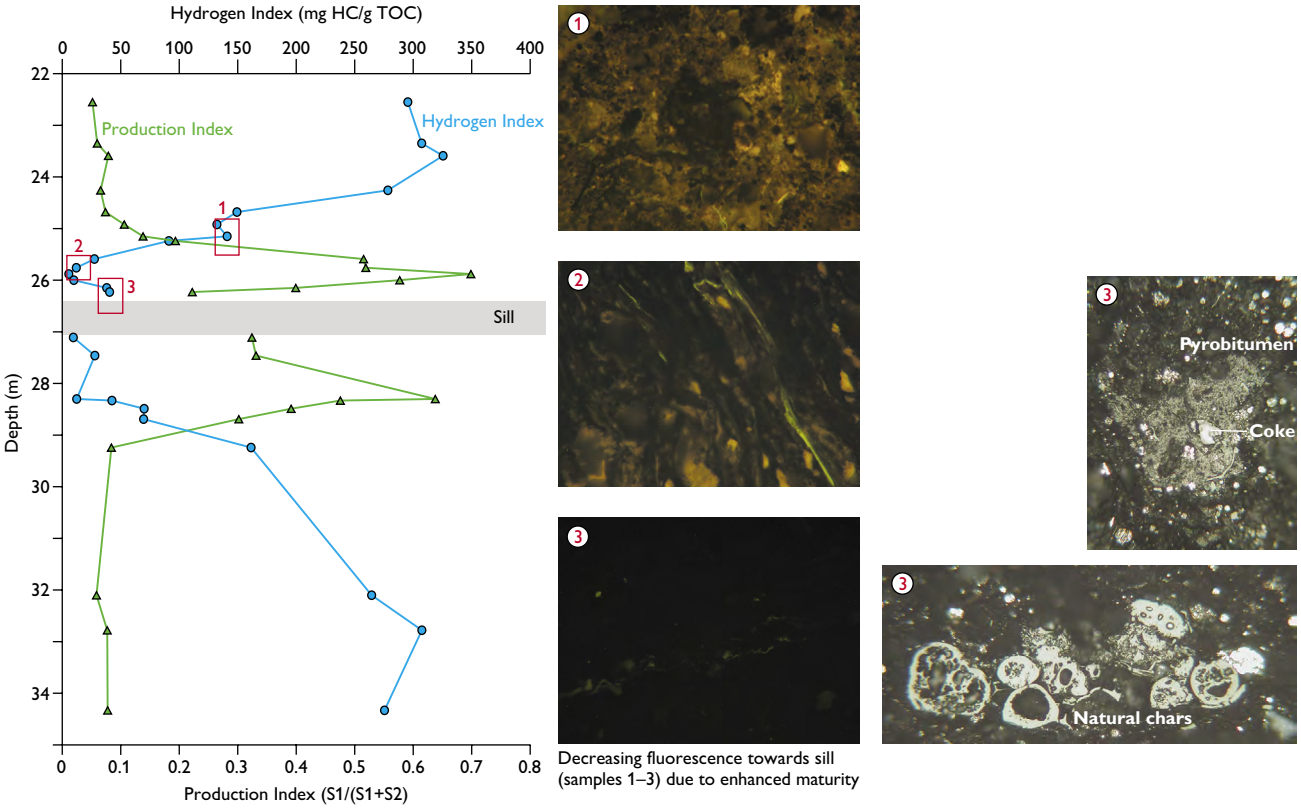

Fig. 13. An example of the effects of magmatic intrusions on the thermal maturity and petroleum potential of adjacent deposits. The petroleum potential of deposits adjacent to magmatic intrusions was rapidly realised, as shown by decreasing HI. The PI increases sharply due to petroleum generation, but closest to the intrusion, the PI decreases again due to cracking and thermal destruction of petroleum to form gaseous components that tended to escape. The fluorescence-intensity of the liptinite group decreased as petroleum was generated (samples 1–3, see cross-plot) and high temperatures immediately adjacent to the intrusions led to the formation of pyrobitumen and natural chars (see sample 3, photos right), whereas some sedimentary coal-particles were transformed to coke.

c. 0.08 in the upper 90 m of the succession, whereas the homohopane ratio increases from a value close to 0.02 to an average of *c*. 0.08 over the same interval. The bisnorhopane ratio shows strong variation but with a rapid increase from a near-zero value at TD to *c*. 1 over the lowermost 60–70 m. The percentage of marine C_{30} steranes (n-propylcholestanes) increases from values close to 3% near TD to values close to 8% in the upper *c*. 90 m of the succession, whereas $\delta^{13}C$ shows a trend from relatively less depleted isotopic compositions (c. –27‰) to more strongly depleted compositions (*c*. –30‰) over the same interval. This feature is even more clearly expressed when the isotopic composition of the total extract is plotted against the pristane to phytane ratio (Fig. 14), where the broad right-to-left trend indicated represents the overall up-section development. Where applicable, data on oil stains collected at 55.4 m and 105.18 m are shown together with rock data. The deeper sample (105.18 m) shows a near-identical composition relative to nearby rock samples in all parameters considered, whereas the shallower sample (55.4 m) shows slight to moderate deviation in some parameters (Fig. 12). Characteristic fingerprints of samples representing the upper (sample 16827, 80.77 m) and lower (sample 16850, 205.84 m) parts of the drilled succession are shown in Fig. 15, and for comparison corresponding data on the two oil stain samples are shown in Fig. 17. A common feature of all samples is low to moderate proportions of rearranged hopanes such as neohopanes and diahopanes, whereas the proportions of rearranged steranes are generally somewhat higher. Relative to samples of the upper part of the succession, samples of the lower part show much higher proportions of long-chain ('waxy') n-alkanes and a much higher pristane/phytane ratio. The entire succession is remarkably low in tricyclic terpanes, but the samples from the deeper part of the succession clearly contain even less than samples

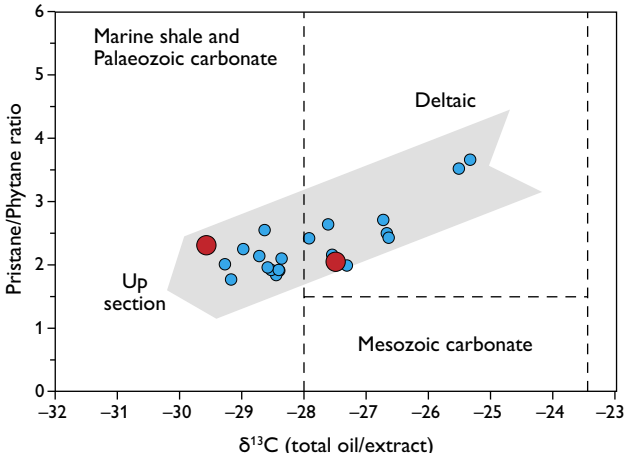

Fig. 14 Blokelv-1 core, stable carbon isotope $\delta^{13}C$ of total extract fractions (calculated by combining extract composition and isotope data for individual fractions) vs. pristane/phytane ratio. Red symbols indicate oil sample (stain) data. Plot after Chung *et al.* (1992). From the base of the core upwards, there is a general right-to-left trend from high pristane/phytane and undepleted $\delta^{13}C$ to lower pristane/phytane and increasingly depleted $\delta^{13}C$, mirroring a facies change from terrestrially influenced kerogen to increasingly marine-dominated kerogen (see text for discussion).

from the upper part. Samples from the upper part of the succession often contain high proportions of 28,30-bisnorhopane, and extended hopanes, whereas samples from the deeper part only contain minor proportions of 28,30-bisnorhopane as well as of extended hopanes. C_{30} n-propylcholestanes are scarce in the lower portion of the succession but increase rapidly in abundance upwards as the overall distribution of steranes changes from a strong predominance of C_{29}-steranes to near-equal proportions of C_{27}, C_{28} and C_{29}-steranes (Fig. 15, Table 6).

The variation of kerogen composition with depth demonstrated by the various organic geochemical parameters mentioned above are clear in the petrographic composition of the kerogens present (Fig. 16). Evidently, the kerogen of the deeper part of the succession is predominantly terrestrial, being composed of vitrinite and inertinite, with only minor proportions of detrital liptinite, presumably alginite, and fluorescent amorphous organic matter. Conversely, the kerogen of the upper part of the succession is predominantly marine, being composed of alginite and fluorescent amorphous organic matter, with only minor proportions of terrestrial constituents such as vitrinite and inertinite.

The shallower oil stain sample collected at 55.4 m, close to the most organic-rich part of the source-rock succession, shows clear signs of biodegradation leading to a marked reduction in the abundance of normal alkanes and a corresponding enhancement of more complex moieties, including hopane and sterane biological markers, which may even be discerned in the GC-FID data (Fig. 17). In addition, a prominent envelope of unresolved complex components is observed. Although individual biological marker ratios may deviate slightly from expected values, the overall characteristics of the sample correspond well to those of nearby source-rock samples. The deeper oil stain sample collected at 105.18 m, *c.* 25 m below the initiation of the change in geochemical characteristics with depth, is largely unaffected by biodegradation but may have suffered minor evaporative losses in the lower boiling point range. In all measured parameters, this sample shows close correlation to neighbouring source-rock samples. Within the entire succession, it occupies an intermediate position, showing characteristics between those of the shallower and deeper parts of the source rock succession (Figs 12, 14, 15, 17, Table 4).

Discussion

Although stratigraphic datings are not available from all outcrop samples, existing evidence indicates that these samples and the 'old boreholes' represent the upper part of the Olympen Formation and the lowermost and the topmost parts of the Katedralen Member (Hareelv Formation), whereas the central parts of the Hareelv Formation are left essentially unsampled (Fig. 3). The Blokelv-1 core provides full coverage of the stratigraphic intervals that were not represented in other sample material as well as of duplicating of the succession that was represented by older core and outcrop samples; note, however, that the Blokelv-1 borehole did not penetrate the base of the Hareelv Formation. In the northern North Sea region, deposition of organic-rich shales continued into the Early Cretaceous (Ryazanian), with the richest and most oil-prone deposits being present in the Upper

Facing page:
Fig. 15. Biological marker data. Characteristic fingerprints of samples representing the upper (sample 16827, 80.77 m) and lower (sample 16850, 205.84 m) parts of the drilled succession. GC-MSMS parent–daughter traces for steranes and hopanes represent the sum of five and nine parent–daughter transitions, respectively.

Sample 16827, 80.77 m

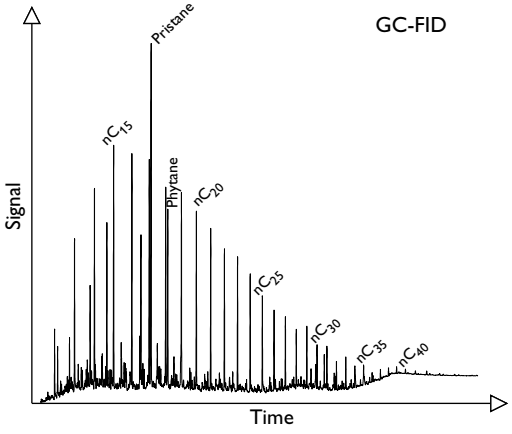

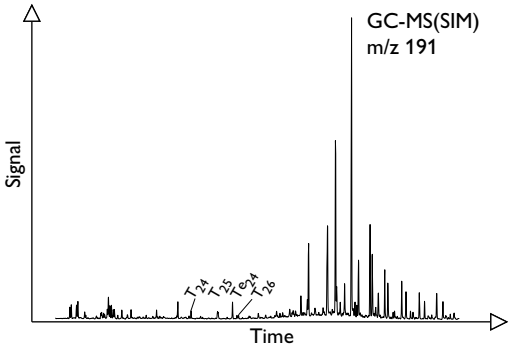

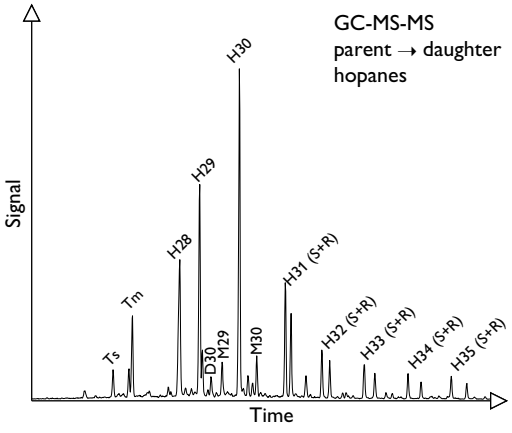

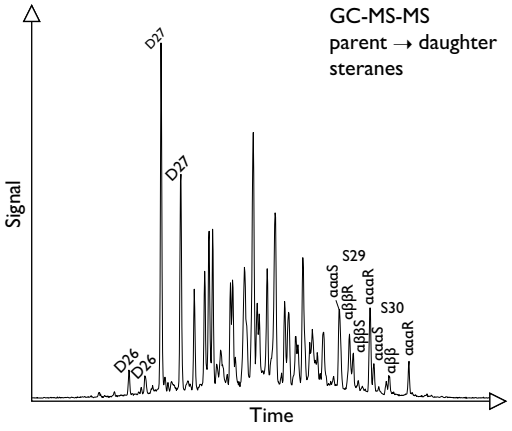

Sample 16850, 205.84 m

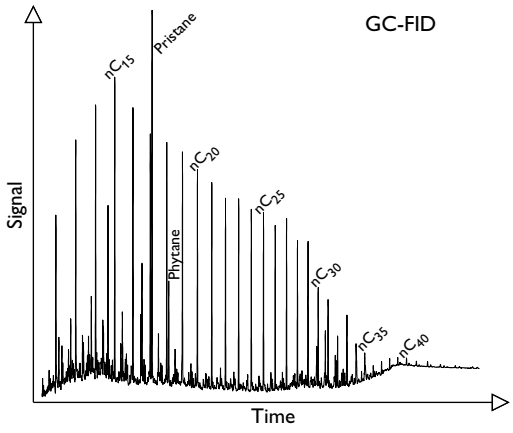

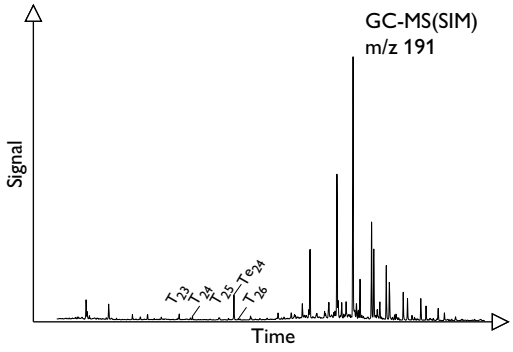

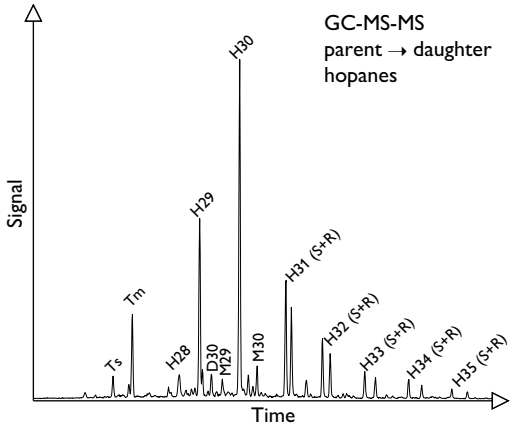

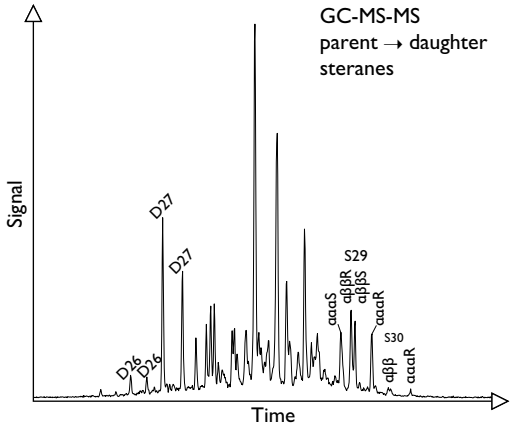

Table 4. Gas chromatography, biomarker and isotopic data on core extracts and oil stains

Sample	Depth (m)	Pr/Ph	BNH/ H30	29Ts	D30	IHR	HHI	S27 (%)	S28 (%)	S29 (%)	S30 (%)	S29 (S/S+R)	S29 ββ/ (ββ+αα	Dia/ (Dia+ Reg)	$\delta^{13}C$ (sat)
511101-107	12.62	2.55	0.17	0.20	0.07	0.06	0.09	28.2	30.1	34.3	7.5	0.35	0.33	0.72	–30.5
511101-110	16.42	2.36	0.92	0.17	0.08	0.06	0.12	29.3	28.8	33.9	8.1	0.37	0.33	0.67	
511101-113	20.15	2.25	0.11	0.19	0.07	0.07	0.09	28.6	30.7	32.6	8.0	0.36	0.34	0.71	–30.6
511101-8	23.59	2.01	0.32	0.13	0.05	0.07	0.07	30.4	32.9	28.4	8.3	0.41	0.33	0.66	–30.2
511101-117	24.26	1.95	0.24	0.12	0.05	0.07	0.07	30.6	32.1	28.5	8.8	0.43	0.34	0.66	
511101-139	24.68	1.88	0.11	0.13	0.05	0.07	0.06	31.5	31.3	28.6	8.6	0.46	0.36	0.66	
511101-118	25.15	1.91	0.08	0.10	0.06	0.07	0.07	32.5	31.3	27.3	8.9	0.50	0.48	0.76	–29.4
511101-137	25.24	1.92	0.01	0.11	0.06	0.07	0.06	34.1	31.6	26.1	8.2	0.54	0.58	0.83	–29.1
511101-119	25.76	1.77													
511101-135	25.88	1.93	0.24	0.13	0.07	0.09	0.07	34.8	31.0	26.6	7.6	0.43	0.44	0.82	
511101-121	26.23	1.84	0.40	0.11	0.08	0.07	0.09	33.1	30.3	28.4	8.1	0.40	0.35	0.67	–29.0
511101-122	27.11	1.86	0.03	0.13	0.10	0.06	0.10	33.9	30.0	28.4	7.7	0.40	0.36	0.69	
511101-141	27.46	1.77	0.40	0.11	0.08	0.07	0.08	33.7	30.4	28.4	7.5	0.42	0.39	0.73	–32.3
511101-123	28.33	1.62													
511101-144	28.69	2.64	0.03	0.08	0.05	0.09	0.04	31.1	28.9	33.8	6.2	0.55	0.58	0.83	–28.9
511101-124	29.24	1.84	0.20	0.11	0.05	0.07	0.08	29.8	32.3	29.2	8.7	0.49	0.43	0.71	
511101-125	32.10	1.92	0.49	0.13	0.06	0.06	0.09	30.8	32.9	28.7	7.5	0.42	0.34	0.65	–30.1
511101-12	32.78	1.96	0.50	0.11	0.05	0.06	0.10	30.0	32.1	29.7	8.3	0.41	0.33	0.68	–30.4
511101-146	50.27	2.06	0.44	0.14	0.07	0.08	0.09	30.4	28.3	32.9	8.4	0.45	0.34	0.66	
511101-150	64.91	2.10	0.66	0.15	0.07	0.06	0.09	30.9	29.9	31.2	8.0	0.46	0.36	0.68	–30.0
511101-24	68.77	1.97	0.38	0.14	0.07	0.07	0.09	33.1	27.9	31.8	7.2	0.47	0.36	0.66	
511101-28	80.77	2.14	0.56	0.13	0.06	0.07	0.09	31.9	28.1	31.1	8.9	0.48	0.37	0.72	–29.7
511101-164	82.14	1.89	0.18	0.16	0.07	0.07	0.10	34.3	27.1	29.8	8.7	0.49	0.40	0.72	
511101-170	89.22	2.42	0.10	0.11	0.06	0.07	0.08	29.2	25.8	38.8	6.2	0.49	0.40	0.74	–29.3
511101-32	92.74	2.36	0.11	0.12	0.06	0.08	0.08	29.5	25.6	39.1	5.8	0.50	0.40	0.74	
511101-174	93.02	2.16	0.27	0.11	0.06	0.08	0.08	30.3	25.3	39.0	5.4	0.50	0.41	0.74	–29.1
511101-175	97.42	1.99	0.07	0.05	0.05	0.08	0.05	35.4	27.1	32.8	4.7	0.55	0.57	0.80	–28.5
511101-176	98.48	2.67	0.40	0.08	0.04	0.10	0.05	32.4	24.4	38.2	5.0	0.46	0.44	0.71	
511101-177	103.98	2.74													
511101-36	104.79	2.43	0.09	0.05	0.03	0.09	0.05	33.3	25.9	36.1	4.6	0.53	0.55	0.77	–28.1
511101-178	105.72	2.50	0.21	0.09	0.03	0.08	0.07	28.6	24.8	41.2	5.4	0.51	0.43	0.72	–28.6
511101-179	106.59	2.71	0.38	0.10	0.05	0.01	0.07	29.7	26.1	38.4	5.8	0.50	0.44	0.74	–28.7
511101-186	117.73	2.60	0.77	0.13	0.07	0.08	0.09	37.7	23.9	31.3	7.1	0.50	0.42	0.75	
511101-195	142.84	3.08	0.40	0.09	0.08	0.09	0.06	28.1	21.7	43.6	6.5	0.52	0.48	0.75	
511101-203	160.80	3.52	0.95	0.08	0.06	0.09	0.05	37.0	17.8	40.9	4.3	0.50	0.52	0.76	–27.1
511101-60	176.77	3.83	0.43	0.13	0.07	0.08	0.05	29.6	20.7	44.5	5.2	0.49	0.53	0.82	
511101-220	205.84	3.66	0.09	0.11	0.07	0.11	0.04	20.8	18.9	56.2	4.1	0.53	0.54	0.78	–27.3
511101-228	232.05	5.77	0.01	0.09	0.09	0.12	0.02	18.2	19.3	59.9	2.7	0.50	0.55	0.84	
Oil stain	105.18	2.31	0.12	0.04	0.03	0.08	0.08	31.0	25.4	38.3	5.2	0.53	0.47	0.75	–28.5
Oil stain	55.4	2.05	0.63	0.09	0.05	0.06	0.14	31.2	25.8	37.1	5.9	0.47	0.37	0.72	–28.5

Pr/Pr: Pristane/Phytane ratio.

BNH/H30: 28,30-bisnorhopane/hopane ratio.

IHR: isohopane ratio (Nytoft 2011).

HHI: Homohopane index (H35/Σ(H31-H35)).

S27 (%), S28 (%), S29 (%), S30 (%): distribution of total C_{27}–C_{30} steranes (diasteranes + regular steranes), normalised to 100%.

S29 (S/(S+R)): C_{29} sterane 20S/(20S+20R) isomer ratio.

S29 ββ/(ββ+αα): C_{29} sterane αββ/(αββ+ααα) isomer ratio.

Dia / (Dia + Reg): total $C_{27–30}$ diasteranes /(total $C_{27–30}$ diasteranes + total $C_{27–30}$ regular steranes).

$\delta^{13}C$ (sat): stable carbon isotopic ratio, saturated fraction.

Volgian – Ryazanian succession (e.g. Ineson *et al*. 2003 and references therein; Justwan *et al*. 2006a). In contrast, most of the corresponding Volgian–Ryazanian succession in Jameson Land is sand-rich, although a few mudstone samples with rather modest petroleum potential have been collected from the Ryazanian Hesteelv Formation in southern Jameson Land. The Hesteelv Formation, which was deposited in an incised valley during the initial phase of regional flooding in the Ryazanian (Surlyk 1973; Surlyk *et al*. 1973; F. Surlyk personal communica-

tion, 2014), represents the youngest Mesozoic deposits in Jameson Land. Despite the muddy nature of the lower Crinoid Bjerg Member of the Hesteelv Formation, the highly oil-prone shales known from the uppermost Volgian – Ryazanian succession in other parts of the greater North Atlantic region seem not to have been deposited in Jameson Land although they are recorded farther north in North-East Greenland.

Outcrop samples

Outcrop samples generally show pre-oil window thermal maturity, except for samples from the Fortet and Katedralen outcrops affected by widespread basaltic intrusions, and are rich in organic matter although their levels of TOC show wide variation. In absolute terms, as represented by the S2-parameter, their petroleum potential is generally good or even excellent, but when normalised by TOC to calculate the Hydrogen Index, the kerogen is classified as primarily gas-prone type III or gas/oil-prone type II/III. Hence, compared to correlative stratigraphic intervals in the greater North Atlantic area, the apparent petroleum potential is surprisingly poor. This may in part be attributed to the high proportions of oxidised and terrestrial organic matter observed in palynological preparations, which may serve to 'downgrade' the Hydrogen Index by adding large amounts of organic carbon that do not participate in petroleum generation. An additional cause may be the very large concentrations of finely disseminated pyritic sulfur present in the shales. Very few analyses of TS have been made on outcrop samples, but systematic analyses of the Blokelv-1 core (Fig. 9) indicate that fresh/unweathered core samples represent the original values of the outcrop samples. Weathering of pyrite will ultimately generate sulfuric acid, which, by its oxidising nature, attacks kerogen and reduces its petroleum potential. Extensive weathering of pyrite is evident on outcrop faces that are commonly encrusted with greenish-yellow jarosite, a potassium-iron sulphate-mineral ($KFe_3+3(OH)_6(SO_4)_2$) characteristically formed by pyrite weathering (Fig. 18). Hence, data on the petroleum potential derived from surface/outcrop samples are not representative if the rocks contain large amounts of finely disseminated pyrite.

'Old boreholes'

These core samples show strongly variable petroleum potential, but only represent a restricted stratigraphic interval since the lower and middle Kimmeridgian intervals were not penetrated. The majority of the samples can be classified as either gas-prone, containing predominantly Type III kerogen, or as non-source deposits containing predominantly inert kerogen. However, a large proportion of the samples shows HI values of 200–300 or higher and may be classified as gas/oil-prone to oil prone. On average, both T_{max} and the Production Index (PI) indicate pre-oil window maturity, but the average values mask widely varying values of both T_{max} and PI, suggesting localised maturation and petroleum generation caused by heating from the abundant intrusions present in the area. Although it is impossible to make a straight comparison due to the stratigraphical and lithological differences, it seems that core samples do show higher average petroleum potential than outcrop samples due to weathering of the latter. In the Sjællandselv-1 and the Jyllandselv-1 cores, assessment of the quality of the reactive kerogen fraction can be ascertained by the linear trendline shown by the TOC vs. S2 plot (Fig. 8). This shows that although there is a very large fraction of inert carbon that does not take part in petroleum generation, the reactive fraction of the kerogen is generally oil and gas to oil prone. This is in close accordance with results from the Blokelv-1 core, although the average proportion of inert carbon is significantly lower.

Blokelv-1 petroleum potential and organic facies variations

Due to its continuous stratigraphy from the middle Oxfordian to the lower Volgian, the Blokelv-1 cored section serves as a reference for all other sampling locations, both outcrops and 'old boreholes'. Moreover, it includes the lower to middle Kimmeridgian interval which, apart from being largely untested by other sampling, constitutes a more prolific petroleum source succession than any other interval known in the Upper Jurassic of Jameson Land.

Based on petroleum geochemical data, it is clear that the succession penetrated by the Blokelv-1 borehole is divided into two subunits (Fig. 9). A lower unit, extending from TD to *c.* 110 m, is characterised by generally high levels of TOC, moderate sulfur content, and high S2-yields, resulting in HI-values slightly below 300 on average, showing a clear upward-increasing trend. These

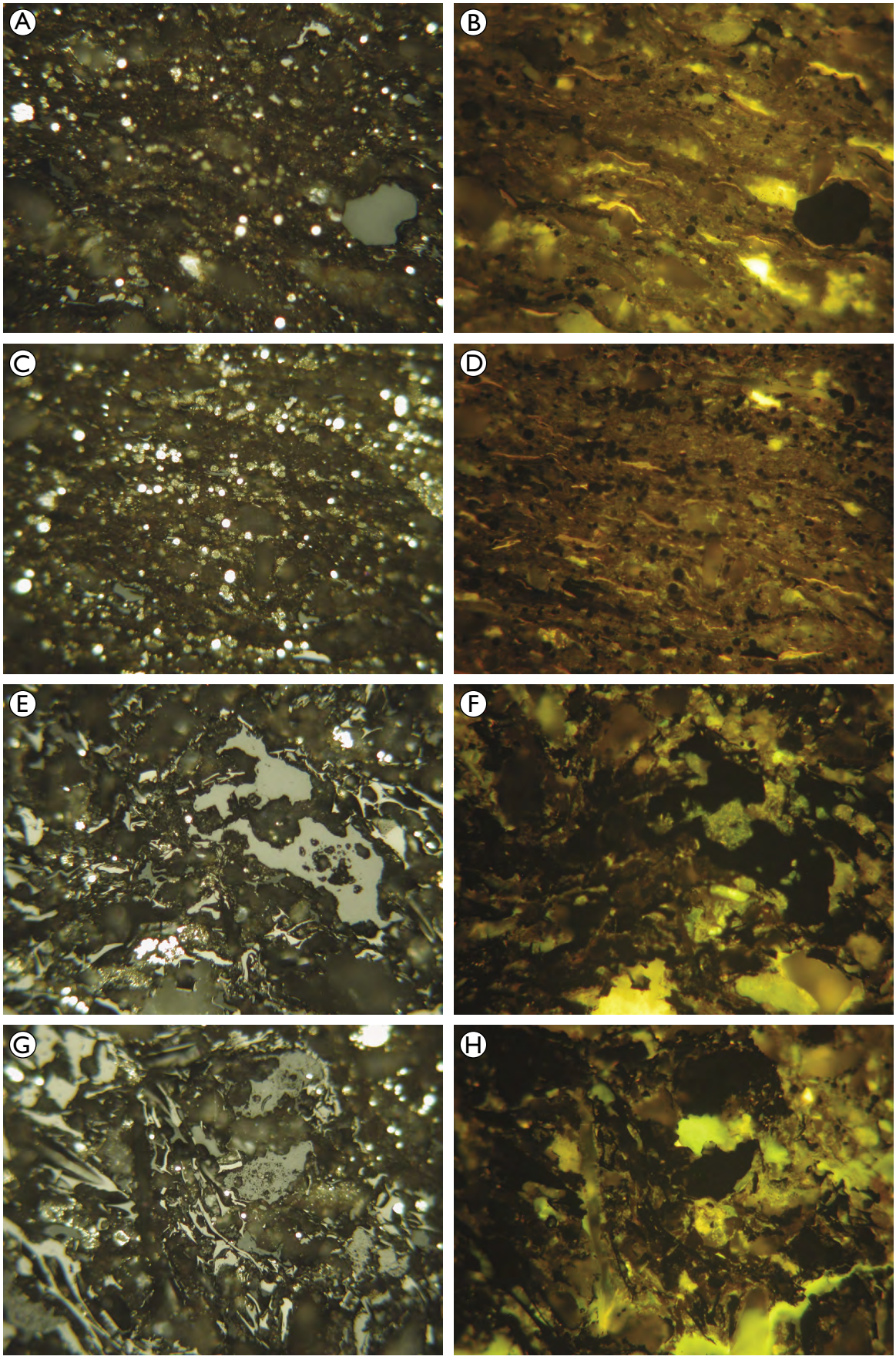
A
B
C
D
E
F
G
H

deposits accumulated during overall rising sea level (Bjerager *et al*. 2018b, c, this volume). The transition to the overlying unit is obscured by an intrusion which has affected the petroleum potential of the adjacent succession both above and below. By comparison, the upper unit from *c*. 90 m to *c*. 10 m is characterised by fairly high levels of TOC, predominantly oil-prone kerogen and very high levels of sulfur, and slightly higher average HI. The unit shows a fairly clear maximum in all parameters over the interval from *c*. 80 m to *c*. 60 m. This interval was deposited during a prominent sea-level highstand (Bjerager *et al*. 2018b, c, this volume). The drilled succession thus records changes in depositional conditions in response to a gradually rising sea level from TD to *c*. 90 m, culminating in the interval 90–60 m; the analytical data suggest a weak regressive trend in the uppermost 60 m of the cored succession.

Although the general depositional environment is marine and strongly oxygen-restricted throughout the succession, the kerogen shows a temporal change from marine with a prominent terrestrial component to compositions with successively less terrestrial organic matter, culminating in the interval 90–60 m (Fig. 16). This trend is also evident from biomarker and isotopic data (Figs 12B, 14), notably pristane/phytane ratios, the proportion of marine C_{30} n-propylcholestanes and $\delta^{13}C$, but also isohopane and homohopane ratios, and even raw data (Fig. 15). Hence, a clearly decreasing trend in pristane/phytane ratio is observed upwards through the succession (Fig. 12B). A similar, but a less pronounced trend is observed in the isohopane ratio, which is a very sensitive indicator of terrestrial organic contributions (Nytoft 2011). Upward-increasing trends are observed in the homohopane ratio, pointing to increasingly oxygen-deficient depositional environments, and in the percentage of C_{30} n-propylcholestanes, pointing to increasing proportions of marine organic matter in the kerogen. Stable carbon isotopic ratios show a clear trend from less depleted to more depleted isotopic compositions, suggesting changing proportions of terrestrial relative to marine kerogen in favour of the latter. Conversely, the 28,30-bisnorhopane ratio does not show any clear trends, but the abundance of 28,30-bisnorhopane is remarkable when compared to equivalent deposits in the North Sea region, where high levels of 28,30-bisnorhopane are characteristic of the uppermost, highly prolific Volgian–Ryazanian part of the succession whereas its abundance in the deeper parts, for instance in the Kimmeridgian succession, is often low (e.g. Ineson *et al*. 2003). Oil-stains recorded at 55.4 m and 105.18 m show biomarker fingerprints reflecting their stratigraphic position in the succession, in that they show characteristics very similar to the shales adjacent to the intrusion in or near which they occur (Figs 12B, 14, 17). The deeper stain shows a near-perfect match to nearby samples whereas the shallower stain shows minor deviation in some parameters, probably related to its biodegraded nature (Fig. 17).

Despite the changes in organic facies documented by a number of independent parameters, oil-prone petroleum source rocks are present throughout the entire drilled succession. Moreover, as indicated by the hydrogen index, the difference in petroleum potential between the more terrestrial lower part and the upper more marine part is trifling. This unexpected observation may have to do with the balance between inert and labile sedimentary organic matter, where the latter can be expected to be 'diluted' by the former, which will then serve to drag down the hydrogen index. Conceivably, the autochthonous marine organic matter is diluted by allochthonous inert material. This effect will be more pronounced the lower the TOC, if the autochthonous contribution is more or less constant. However, based on the geochemical signature of the oil-stains found, it is clear that even the terrestrial fraction of the kerogen in the lower part of the succession is oil prone since both stains show clear relationships to the shales immediately adjacent to them.

Facing page:

Fig. 16. Examples of kerogen composition in the upper (A–D) and lower (E–H) parts of the drilled succession. Polished block preparations, reflected light microscopy, horizontal edge of photographs is *c*. 300 micron. **Photos A–D from sample 16827 (81 m)**. **A**: Finely laminated mudstone, abundant framboidal pyrite (bright white) and vitrinite (grey). **B**: Same field as A, fluorescence-inducing blue light. Bright yellow alginate, brownish-yellow fluorescing amorphous organic matter. **C**: Finely laminated mudstone, abundant framboidal pyrite (bright white), small vitrinite particles (grey). **D**: Same field as C, fluorescence-inducing blue light. Bright yellow alginate, brownish-yellow fluorescing amorphous organic matter. **Photos E–H from sample 16838 (213 m)**. **E**: Mudstone, containing abundant vitrinite (grey) and inertinite (white), minor amounts of framboidal pyrite (bright white). **F**: Same field as E, mudstone, scattered brownish-yellow fluorescing amorphous organic matter and minute detrital liptinite, presumably alginite. **G**: Mudstone, containing abundant vitrinite (grey) and inertinite (white), minor amounts of framboidal pyrite (bright white). **H**: Same field as G, mudstone, scattered brownish-yellow fluorescing amorphous organic matter and minute detrital liptinite, presumably alginite.

Sample 16053, 55.4 m

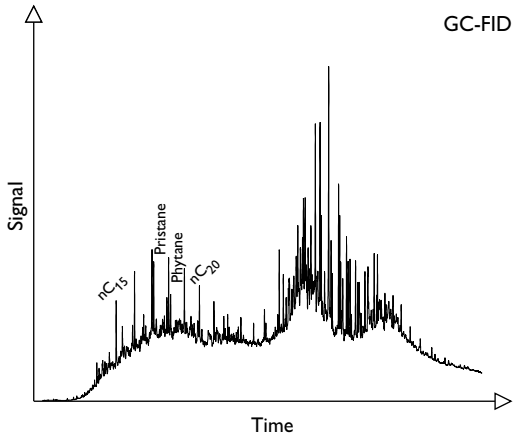

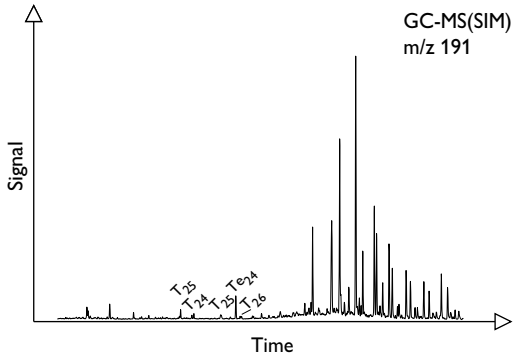

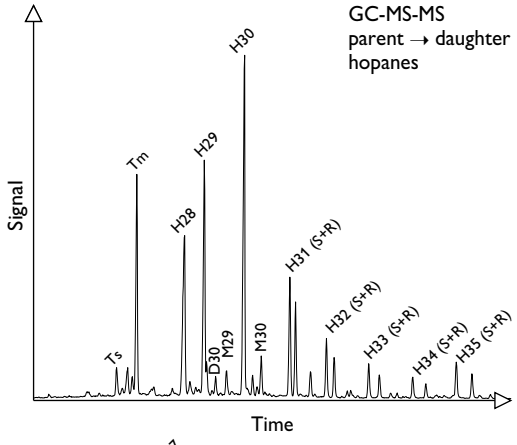

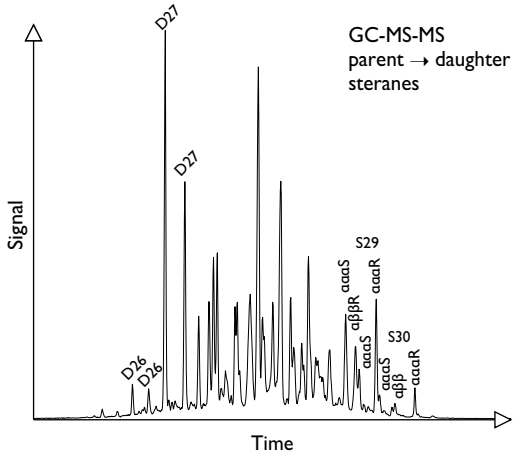

Sample 16764, 105.18 m

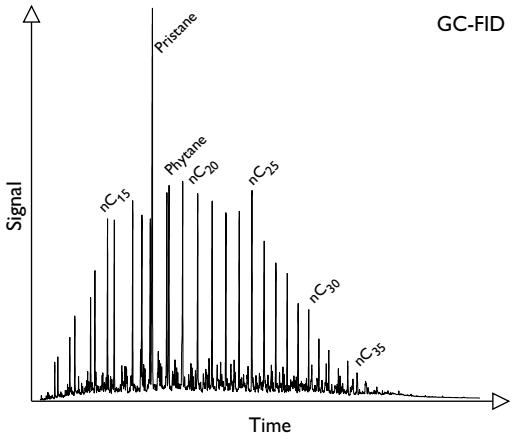

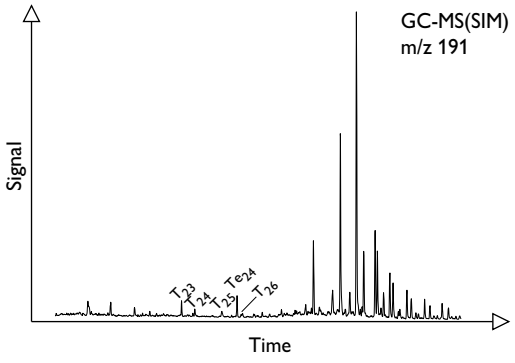

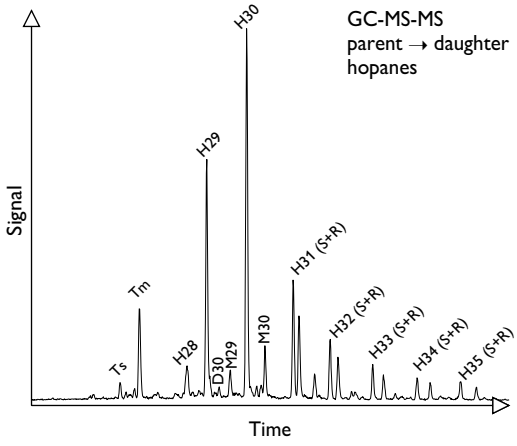

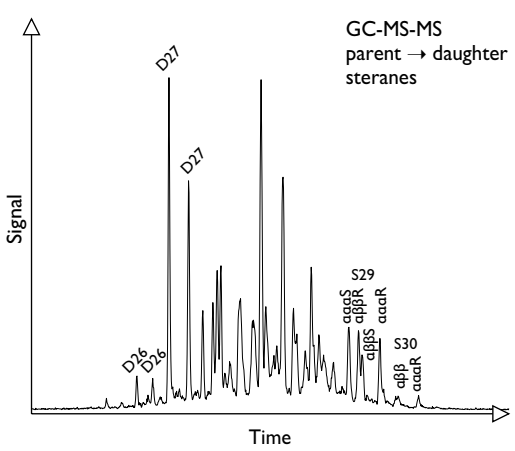

Hence, the above issue is not solely a matter of the balance between labile marine kerogen and more or less inert autochthonous kerogen, but includes qualitative changes in the labile kerogen as well. Systematic organic petrographic data may perhaps shed some light on this matter, but in the absence of such data no acceptable explanation can be offered.

Blokelv-1 borehole thermal maturity

The magmatic intrusions present within the drilled succession have clearly had a significant impact on the thermal maturity of the shales immediately adjacent to them (Fig. 13), where the petroleum potential is rapidly realised, as shown by decreasing HI. Approaching the intrusion, the PI increases sharply recording petroleum generation, but immediately adjacent to the intrusion, the PI decreases in response to cracking and thermal destruction of petroleum to form gaseous components that tend to escape. The fluorescence intensity of liptinite-group macerals decreases as petroleum is generated and high temperatures immediately next to the intrusions led to the formation of pyrobitumen and natural chars, whereas sedimentary coal-particles may form coke. These effects are clearly local, however, and have little influence on the overall level of thermal maturity of the section.

In general, the level of thermal maturity of the Blokelv-1 succession is within the early stages of the oil-generative window, with incipient petroleum generation actually taking place, and in the vicinity of magmatic intrusions the petroleum potential has been more or less realised as evidenced by the presence of oil-stains. Independent thermal maturity indicators such as T_{max} from Rock-Eval type pyrolysis, vitrinite reflectance (%R_o) and biomarker data such as sterane isomerisation ratios and the diasterane ratio are all in perfect agreement, although the latter is also strongly facies-dependant (Fig. 12A, Tables 4, 5, 6). A remarkable feature is the clearly increasing trend with depth observed in all the parameters mentioned, with the transition to the 'oil-window' as defined by T_{max} > 435°C and Ro >0.55% located somewhere in the interval between 120 m and 160 m. A clear gradient is unexpected over such a narrow depth interval (*c.* 234 m). It is evident that a significant thickness of overburden has been removed by erosion since the deposits were at their maximum depth of burial. It is estimated that 2–3 km of Cretaceous-age sediments and Palaeogene-age volcanics have been removed due to Neogene uplift and erosion (Mathiesen *et al.* 1995, 2000; Green & Japsen 2018, this volume). Hence, with a removed section amounting to 2–3 km, the Upper Jurassic succession was close to or within the oil-generative window at its maximum depth of burial, given a modest enhancement of the geothermal gradient as is to be expected from the volcanic activity in the area at the time of maximum burial. Moreover, the abundance of sands intercalated with the shales can conceivably be expected to have served to assist thermal maturation by facilitating fluid movement and thus overcoming time-lag effects caused by differences in thermal conductivity. The processes associated with thermal maturation and the conversion of kerogen into petroleum are not linear but include several 'thresholds', which in coal-petrographic nomenclature are known as 'coalification jumps' (see discussion in Taylor *et al.* 1998), and defined by initiation or rapid changes in the rates of certain processes. Incipient petroleum generation or the start of the 'oil window' coincides with the first 'coalification jump' where a number of processes associated with petroleum generation accelerate, causing the non-linearity of matu-

Fig. 18. Outcrop of the Katedralen Member shales near the Blokelv-1 drill site, showing widespread coating by jarosite (orange–yellow) formed from weathering of pyrite.

Facing page:

Fig. 17. Biological marker data. Characteristic fingerprints of oil-stain samples, sample 16053 (55.4 m) and sample 16764 (105.18 m). GC-MS-MS parent–daughter traces for steranes and hopanes represent the sum of five and nine parent–daughter transitions, respectively.

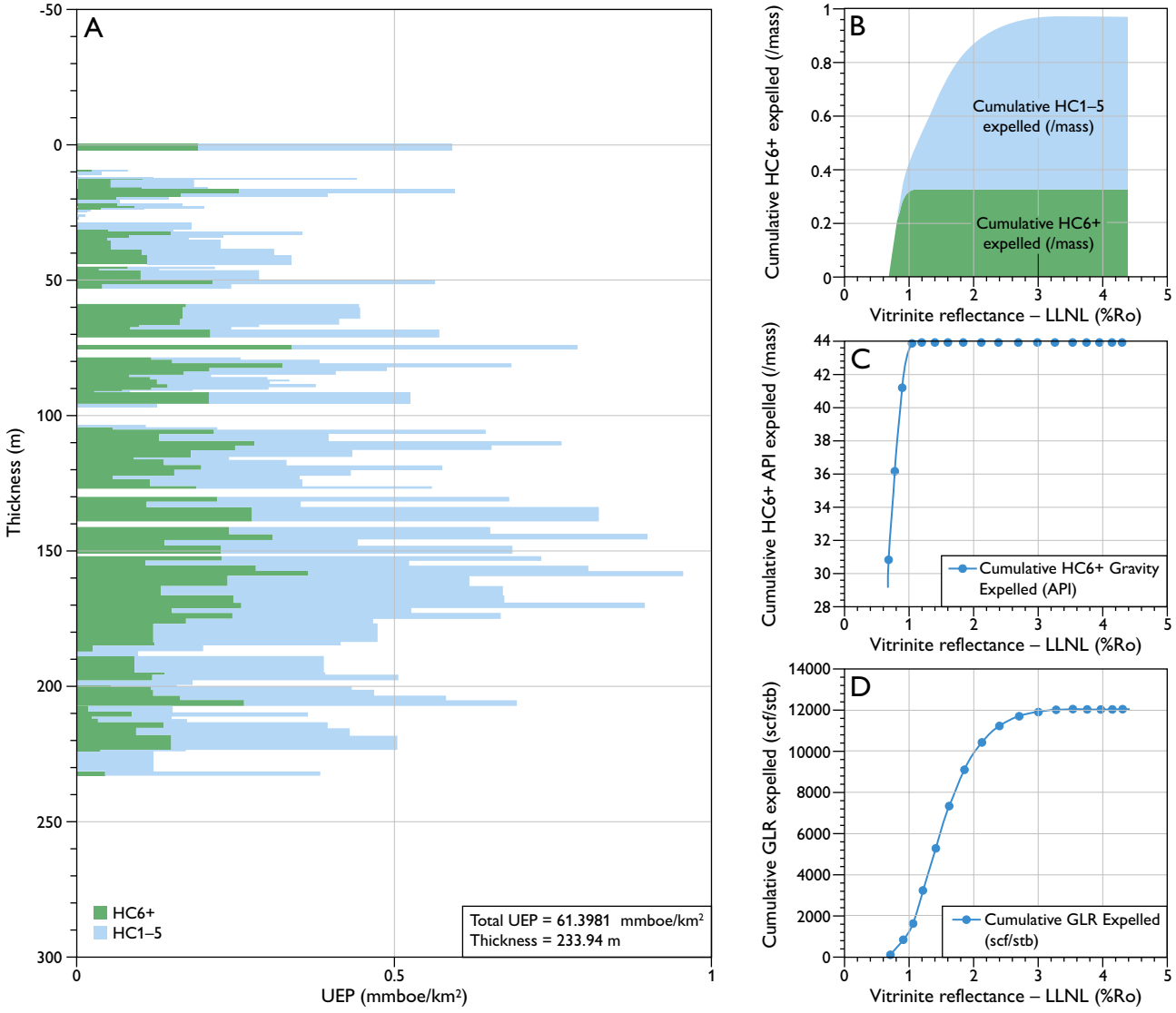

Fig. 19. Calculation of the 'Ultimate Expulsion Potential' (UEP) by Kinex™-modelling results. **A**: Ultimate Expulsion Potential (UEP) vs. depth showing an oil- and gas-prone mudstone section with a total UEP of about 61.4 mmboe/km^2, but with a potential for generation of approximately twice as much gas as oil. **B**: Cumulative expelled C_{6+} hydrocarbons (oil) and C_{1-5} hydrocarbons (gas). Oil generation occurs from about 0.7–1.1% vitrinite reflectance. **C**: Cumulative expelled C_{6+} oil gravities (API) if the mudstones passed through the oil window. The API range suggests generation of medium to light oil. **D**: Cumulative expelled GLR (gas-liquid ratio).

ration profiles observed in exploration wells entering or penetrating the oil generative window. The observed thermal maturity of the Blokelv-1 succession straddles the transition to the oil-generative window, but generation ceased due to uplift and erosion, removing the overlying succession, hence the unusual gradient in particular at depths greater than *c.* 120 m.

Blokelv-1 core: calculation of Ultimate Expulsion Potential (KinEx™ modelling)

Ultimate expulsion potential modelling based on the succession penetrated by the Blokelv-1 borehole calls for caution since both in terms of organic facies variations and thickness of the succession modelled, the basin is not very well constrained. The Blokelv-1 borehole is merely a point-source of information, and caution should be exer-

cised in extrapolating the modelling results to a more regional scale, although for simple comparison with similar successions in the North Atlantic region, such modelling may still be meaningful. The HI and TOC values show that the petroleum generation potential varies through the Blokelv-1 well, which reflects organofacies variations in the marine mudstones. A method to monitor these variations in a more quantitative way is to estimate the potential charged fluid phases (oil and gas) through the mudstone section by calculating the Ultimate Expulsion Potential (UEP; mmboe/km^2). UEP displays the ultimate expellable volume of hydrocarbons in million barrels of oil equivalents (mmboe) per km^2. The KinEx™ tool (Zetaware™) was used to calculate the UEP and to carry out simple maturation modelling of the marine mudstones using a default heating rate of 2°C/Ma and the kinetics of Organofacies B (marine clay-rich shale) as defined by Pepper & Corvi (1995). A depth profile of the UEP calculated from the measured TOC and HI values is shown in Fig. 19A. Calculation of UEP is affected by the thickness of the individual sample intervals. This means that a sample representing a comparatively thick interval will yield a disproportionate large UEP compared to regular thin interval samples. A profile of UEP may therefore be influenced by irregular core sampling intervals resulting in contrasting thicknesses used for the calculations. To overcome this problem and obtain a more representative UEP profile through the mudstone section in Blokelv-1, the *c*. 234 m thick section was subdivided into intervals each *c*. 1–2m thick. Most sample intervals were within this range, thus only a limited number of samples were affected. For example, a 2.4 m thick interval was divided into two subsections of 1.2 m, each interval being assigned the TOC and HI values of the corresponding original sample. The Blokelv-1 well drilled a number of basaltic intrusions and these intervals were assigned TOC and HI values of zero.

The total (cumulative) UEP is *c*. 61.4 mmboe/km^2, but varies through the succession in response to the varying TOC and HI values. This number is in good agreement with estimates of the potential of other Kimmeridge Clay Formation (KCF) equivalent successions in the North Sea and Siberia (Demaison & Huizinga 1991) even though the Blokelv-1 core represents only a fraction of the total thickness of the KCF-equivalent succession. The igneous intrusions and the adjacent mudstones with overcooked kerogen are clearly identified by the gaps in the profile with no potential. Sandstone beds have not been subtracted from the UEP calculation, and the total UEP is thus a maximum estimate, since the KinEx™ tool cannot accommodate the full complexity of the interbedded mudstone–sandstone succession. The lower part of the cored section has a fluctuating oil potential, but a higher capacity to generate and expel gas, so although the mudstones have a propensity to generate both oil and gas, they are primarily gas-prone. The oil generation potential increases up-section and is at a maximum in the interval 175–130 m, a trend followed by the gas generation potential (Fig. 19A). Above 130 m, the oil generation potential decreases, attaining a relatively stable level from 130 m to 70 m, above which point it decreases progressively up-section. The UOP (Ultimate Oil Potential) is *c*. 20 mmboe/km^2 whereas the UGP (Ultimate Gas Potential) is *c*. 41.4 mmboe/km^2, i.e. a substantially higher proportion of gas than oil will be generated. The KinEx™ model predicts that on passing through the oil window, the mudstones will generate C_{6+} hydrocarbons from *c*. 0.7%R_o to slightly above 1%R_o with a cumulative API ranging from *c*. 29° to *c*. 44° (Figs 19B, C). The charge up to a vitrinite reflectance of about 1.1–1.2%R_o will be 'black' to 'volatile' oil with a GLR (Gas-liquid ratio) of less than 3000 scf/stb (Fig. 19D). Further maturation would result in wet gas/condensate generation.

Regional implications

The documentation of a rich gas/oil-prone Upper Jurassic succession in Jameson Land is obviously important for the assessment of the regional petroleum potential, including the North-East Greenland continental shelf, the Jan Mayen area and perhaps also areas onshore Greenland. In Jameson Land, the source-rock succession is intimately associated with potential reservoir rocks constituted by the various types of gravity-flow sands and injectites that make up more than 40% of the cored sequence, but the succession is near the surface or exposed over most of the area. However, the basin is gently tilted towards the south and seismic data indicate that the sedimentary succession continues under Scoresby Sund and the thick basaltic cover of the Volquart Boon Kyst that faces Jameson Land from the south (Larsen 1980). Hence, a conceptual play could be developed, based on the intimate association of a rich gas/oil-prone source rock and interleaved units of sandstone showing good reservoir quality, sealed by overlying Cretaceous–Palaeogene mudstones and Palaeogene volcanics. The Cretaceous–Palaeogene succession has been largely removed in Jameson Land during subsequent uplift (Mathiesen *et al*. 1995, 2000; Green & Japsen 2018, this volume), but in areas south of

Jameson Land and perhaps elsewhere in comparable settings it may have been preserved. Such a play constitutes a variant of the synrift play demonstrated by the Pil and Bue discoveries on the Halten Terrace in the Norwegian offshore. In the present case, stacked synrift sands act as reservoirs, separated by rich source rocks of the Hareelv Formation, equivalent to the Melke and Spekk Formations in the Norwegian example, which act as both source rocks and internal seals.

Conclusions

The Upper Jurassic succession of Jameson Land includes a rich gas/oil-prone succession of marine black shales of Oxfordian to early Volgian age, deposited in deep shelfal oxygen-deficient environments that frequently received sandy gravity flows from shallower coastal areas. Palaeogene basaltic intrusions of various sizes are commonly present. The deposits represent the local equivalents to the Kimmeridge Clay Formation *sensu lato* known as the most important petroleum source-rock succession in the greater North Atlantic region, and also in basins east of Canada and in western Siberia.

Outcrop samples have proven largely useless for assessment of petroleum potential because of intense weathering and alteration of the kerogen, probably due to sulfuric acid generated from the breakdown of abundant disseminated pyrite.

The Lollandselv-1, -2, Falsterelv-1 and Jyllandselv-1 fully cored boreholes together cover the lower Oxfordian to lower Kimmeridgian succession below, and overlapping with, the lower part of the Blokelv-1 borehole succession. The deposits are characterised by high contents of terrestrial and inert organic matter but the reactive fraction of the kerogen has the capacity to generate both oil and gas. The Sjællandselv-1, -2 and -3 fully cored boreholes partially overlap stratigraphically and together exhibit the uppermost Kimmeridgian – lower Volgian succession. The petroleum potential varies widely from zero to high for both oil and gas. Although the succession seems to be developed in sandier facies and thus shows lower proportions of mudrocks, its character with respect to petroleum potential seems to match the corresponding part of the Blokelv-1 borehole succession fairly well.

Due to its stratigraphic completeness and coverage from the middle Oxfordian to the lower Volgian – including Kimmeridgian sea-level highstand deposits not represented elsewhere – the Blokelv-1 fully cored borehole (TD 233.8 m) serves as the reference for the entire succession. The succession penetrated by the Blokelv-1 borehole consists predominantly of mudrocks (55%) and, based on petroleum potential/organic facies, the succession may be subdivided into two subunits, albeit the exact transition is obscured by the presence of a magmatic intrusion. The lower unit, extending from TD to *c.* 110 m, is characterised by high levels of TOC, moderate sulfur content, good S2-yields and hydrogen index values slightly below 300 on average, with a clear upwards-increasing trend. These deposits accumulated during an overall rising sea level. The upper unit, showing fairly high levels of TOC, predominantly oil-prone kerogen and very high levels of sulfur, and HI slightly above 300 on average, covers the interval from *c.* 90 m to 10 m with a maximum in most parameters in the interval 60–80 m. The sediments were deposited during a prominent sea-level highstand.

The succession thus records changing depositional conditions in response to an overall rising sea level from TD to *c.* 90 m, culminating in the interval 90–60 m, probably with a regressive tendency in the uppermost portion of the succession. The general depositional environment was marine and oxygen-restricted throughout the succession, but the kerogen facies changes from marine with a prominent terrestrial component towards increasingly marine compositions, culminating in the interval 90–60 m. This development is also recorded by a number of biological marker parameters as well as by the stable carbon isotopic ratio ($\delta^{13}C$).

Oil stains recorded in association with magmatic intrusions show biological marker fingerprints very similar to the shales adjacent to the intrusions, testifying to their local origin. Hence, the intrusions have had a profound effect on the thermal maturity of adjacent rocks, but the effects are local and restricted to a fairly narrow zone below and above the intrusions. The characteristics of the oils fall well within the range of variation seen in oils generated from correlative successions elsewhere in the greater North Atlantic region. A series of thermal maturity indicators (R_o, T_{max}, biological markers) consistently show unexpected increasing depth-trends within only about 200 m of stratigraphic thickness. The thermal maturity of the Blokelv-1 succession straddles the transition to the oil-generative window where a number of geochemical processes accelerate, and the trend in thermal maturity probably represents quenching of incipient petroleum generation by rapid Neogene uplift after maximum depth of burial was reached in the Palaeogene.

Calculation of the 'Ultimate Expulsion Potential' (UEP) by KinEx™ modelling suggests that although the kerogen in general is classified as gas/oil-prone, ultimately about twice as much gas as oil would be generated from

the succession. The UEP is unevenly distributed throughout the drilled succession with a maximum in the interval *c*. 170–130 m despite the lower average HI of this interval, when compared to the sea-level highstand succession above. A maximum estimate of the Ultimate Expulsion Potential (UEP) amounts to 61.4 mmboe/km^2, which is in close agreement with published estimates of correlative successions in the greater North Atlantic region.

The documentation of a rich gas/oil-prone Upper Jurassic succession in Jameson Land is important for the assessment of the regional petroleum potential, including the North-East Greenland continental shelf, the Jan Mayen area and perhaps also areas onshore Greenland, where a new conceptual play may be defined that represents a variant of the 'synrift sand play' demonstrated by the Pil and Bue discoveries on the Norwegian shelf.

Acknowledgments

We wish to thank Finn Surlyk for helpful comments on an earlier version of this paper. The referees Iain C. Scotchman and Erdem Idiz are thanked for their highly useful and very constructive reviews. Analytical work by Ditte Kiel-Dühring and Carsten Guvad is gratefuly acknowledged, as is draftwork by Jette Halskov and Stefan Sølberg.

References

Alsen, P. & Piasecki, S. 2018: Biostratigraphy of the Hareelv Formation (Upper Jurassic) in the Blokelv-1 core, Jameson Land, central East Greenland. In: Ineson, J. & Bojesen-Koefoed, J.A. (eds): Petroleum geology of the Upper Jurassic – Lower Cretaceous of East and North-East Greenland: Blokelv-1 borehole, Jameson Land Basin. Geological Survey of Denmark and Greenland Bulletin **42**, 15–37 (this volume).

Birkelund, T. & Perch-Nielsen, K. 1976: Late Palaeozoic – Mesozoic evolution of central East Greenland. In: Escher, A. & Watt, W.S. (eds): Geology of Greenland 304–339. Copenhagen: Geological Survey of Greenland.

Bjerager, M., Alsen, P. Bojesen-Koefoed, J.A., Piasecki, S. & Pilgaard, A. 2018c: Late Jurassic evolution of the Jameson Land Basin, East Greenland – implications of the Blokelv-1 borehole. In: Ineson, J. & Bojesen-Koefoed, J.A. (eds): Petroleum geology of the Upper Jurassic – Lower Cretaceous of East and North-East Greenland: Blokelv-1 borehole, Jameson Land Basin. Geological Survey of Denmark and Greenland Bulletin **42**, 149–168 (this volume).

Bjerager, M., Kjøller, C., Olivarius, M., Olsen, D. & Schovsbo, N. 2018b: Sedimentology, geochemistry and reservoir properties of Upper Jurassic deep marine sediments (Hareelv Formation) in the Blokelv-1 borehole, Jameson Land Basin, East Greenland. In: Ineson, J. & Bojesen-Koefoed, J.A. (eds): Petroleum geology of the Upper Jurassic – Lower Cretaceous of East and North-East Greenland: Blokelv-1 borehole, Jameson Land Basin. Geological Survey of Denmark and Greenland Bulletin **42**, 39–64 (this volume).

Bjerager, M., Piasecki, S. & Bojesen-Koefoed, J. A. 2018a: The Upper Jurassic Blokelv-1 cored borehole in Jameson land, East Greenland – an introduction. In: Ineson, J. & Bojesen-Koefoed, J.A. (eds): Petroleum geology of the Upper Jurassic – Lower Cretaceous of East and North-East Greenland: Blokelv-1 borehole, Jameson Land Basin. Geological Survey of Denmark and Greenland Bulletin **42**, 7–14 (this volume).

Chakhmakhchev, A., Sampei, Y. & Suzuki, N. 1994: Geochemical characteristics of oils and source rocks in the Yamal peninsula, West Siberia, Russia. Organic Geochemistry **22**, 311–322.

Christiansen, F.G., Dam, G., Piasecki, S. & Stemmerik, L. 1992: A review of Upper Palaeozoic and Mesozoic source rocks from onshore East Greenland. In: Spencer, A.M. (ed.): Generation, accumulation and production of Europe's hydrocarbons II. Special Publication of the European Association Petroleum Geologists **2**, 151–161.

Christiansen, F.G., Larsen, H.C., Marcussen, C., Piasecki, S. & Stemmerik, L. 1993: Late Palaeozoic plays in East Greenland. In: Parker, J.R. (ed.): Petroleum Geology of Northwest Europe: Proceedings of the 4th Conference, 657–666. Geological Society, London.

Chung, H.M., Rooney, M.A., Toon, M.B. & Claypool, G.E. 1992: Carbon isotope composition of marine crude oils. AAPG Bulletin **76**, 1000–1007.

Dahl, B., Bojesen-Koefoed, J.A. Holm, A., Justwan, H., Rasmussen, E. & Thomsen, E. 2004: A new approach to interpreting Rock-Eval S2 and TOC data for kerogen quality assessment. Organic Geochemistry **35**, 1461–1477.

Dam, G., Surlyk, F., Mathiesen, A. & Christiansen, F.G. 1995: Exploration significance of lacustrine forced regressions of the Rhaetian–Sinemurian Kap Stewart Formation, Jameson Land, East Greenland. In: Steel, R.J. *et al*. (eds): Sequence Stratigraphy on the Northwest European Margin. Norwegian Petroleum Society Special Publications **5**, 511–527.

Demaison, G. & Huizinga, B.J. 1991: Genetic Classification of petroleum systems. AAPG Bulletin **75**(10), 1626–1643.

Fowler, M.G. & McAlpine, K.D. 1995: The Egret Member, a prolific Kimmeridgian source rock from offshore eastern Canada. In: Katz, B.J. (ed.) Petroleum Source Rocks, 111–130. Berlin: Springer-Verlag.

Green, P.F. & Japsen, P. 2018: Burial and exhumation history of the Jameson Land Basin, East Greenland, estimated from thermochronological data from the Blokelv-1 core. In: Ineson, J. & Bojesen-Koefoed, J.A. (eds): Petroleum geology of the Upper Jurassic – Lower Cretaceous of East and North-East Greenland: Blokelv-1 borehole, Jameson Land Basin. Geological Survey of Denmark and Greenland Bulletin **42**, 133–147 (this volume).

Hamann, N.E, Whittaker, R.C. & Stemmerik, L. 2005: Geological development of the Northeast Greenland Shelf. In: Doré, A.G. & Vining, B.A. (eds): North-West Europe and Global Perspectives – Proceedings of the 6th Petroleum Geology Conference, 887–902. Geological Society, London.

Ineson, J.R., Bojesen-Koefoed, J.A., Dybkjær, K. & Nielsen, L.H. 2003: Volgian–Ryazanian 'hot shales' of the Bo Member (Farsund Formation) in the Danish Central Graben, North Sea: stratigraphy, facies and geochemistry. Geological Survey of Denmark and Greenland Bulletin **1**, 403–436.

Isaksen, G.H & Ledje H.I. 2001: Source rock quality and hydrocarbon migration pathways within the greater Utsira High area, Viking Graben, Norwegian North Sea. AAPG Bulletin **85**(5), 861–883.

Justwan, H. & Dahl, B. 2005. Quantitative hydrocarbon potential mapping and organofacies study in the Greater Balder Area, Norwegian North Sea. In: Doré, A.G. & Vining, B.A. (eds): North-West Europe and Global Perspectives – Proceedings of the 6th Petroleum Geology Conference, 1317–1329. Geological Society, London.

Justwan, H., Dahl, B., Isaksen, G.H. & Meisingset, I. 2005: Late to Middle Jurassic source facies and quality variations, South Viking Graben, North Sea. Journal of Petroleum Geology **28**(3), 241–268.

Justwan, H., Dahl, B. & Isaksen, G.H. 2006a: Geochemical characterisation and genetic origin of oils and condensates in the South Viking Graben, Norway. Marine and Petroleum Geology **23**(2), 213–239.

Justwan, H., Meisingset, I., Dahl, B. & Isaksen, G.H. 2006b: Geothermal history and petroleum generation in the Norwegian South Viking Graben revealed by pseudo-3D basin modelling. Marine and Petroleum Geology **23**(8), 791–819.

Klemme, H.D. 1994: Petroleum systems of the World involving Upper Jurassic source rocks. In: Magoon, L.B & Dow, W.G (eds): The petroleum system from source to trap. AAPG Memoir **60**, 51–72.

Larsen, B. 1980: A marine geophysical survey of the continental shelf of East Greenland 60–71 degrees North (Project Dana 79), 33 pp. + appendix. Copenhagen: Preliminary Report, Geological Survey of Greenland.

Larsen L.M. 2018: Igneous intrusions in the cored Upper Jurassic succession of the Blokelv-1 core, Jameson Land Basin, East Greenland. In: Ineson, J & Bojesen-Koefoed, J.A. (eds): Petroleum geology of the Upper Jurassic – Lower Cretaceous of East and North-East Greenland: Blokelv-1 borehole, Jameson Land Basin. Geological Survey of Denmark and Greenland Bulletin **42**, 127–132 (this volume).

Mathiesen, A., Bidstrup, T. & Christiansen, F.G. 2000: Denudation and uplift history of the Jameson Land basin, East Greenland – constrained from maturity and apatite fission track data. Global and Planetary Change **24**(3–4), 275–301.

Mathiesen A., Christiansen, F.G., Bidstrup, T., Marcussen, C., Dam, G., Piasecki, S. & Stemmerik, L. 1995: Modelling of hydrocarbon generation in the Jameson Land Basin, East Greenland. First Break **13**(8), 329–340.

Miller, R.G. 1990: A paleoceanographic approach to the Kimmeridge Clay Formation. In: Huc, A.Y. (ed.): Deposition of organic facies. AAPG Studies in Geology **30**, 13–26.

Morgans-Bell, H.S., Coe, A.I., Hesselbo, S.P., Jenkyns, H.C., Weedon, G.P., Marshall, J.E.A., Tyson, R.V. & Williams, C.J. 2001: Integrated stratigraphy of the Kimmeridge Clay Formation (Upper Jurassic) based on exposures and boreholes in south Dorset, UK. Geological Magazine **138**(5), 511–539.

Nytoft, H.P. 2011: Novel side chain methylated and hexacyclic hopanes: identification by synthesis, distribution in a worldwide set of coals and crude oils and use as markers for oxic depositional environments. Organic Geochemistry **42**(5), 520–539.

Pepper, A.S. & Corvi, P.J. 1995: Simple kinetic models of petroleum formation. Part I: oil and gas generation from kerogen. Marine and Petroleum Geology **12**(3), 291–319.

Petersen, H.I., Nytoft, H.P., Vosgerau, H., Andersen, C., Bojesen-Koefoed, J.A. & Mathiesen, A. 2010: Source rock quality and maturity and oil types in the NW Danish Central Graben: implications for petroleum prospectivity evaluation in an Upper Jurassic sandstone play area. In: Vining, B.A. & Pickering, S.C. (eds): Petroleum Geology: From mature basins to new frontiers – Proceedings of the 7th Petroleum Geology Conference, 95–111. Geological Society, London.

Pilgaard, A. 2012: Unikke sandede tyngdestrømsaflejringer og injektitter i Øvre Jura, Jameson Land, Østgrønland, 98 pp. Unpublished MSc thesis, University of Copenhagen, Denmark (in Danish).

Radke, M., Willsch, H. & Welte, D.H. 1980: Preparative hydrocarbon group determination by automated medium pressure liquid chromatography. Analytical Chemistry **52**(3), 406–411.

Requejo, A.G., Hollywood, J. & Halpern, H.I. 1989: Recognition and source correlation of migrated hydrocarbons in Upper Jurassic Hareelv Formation, Jameson Land, East Greenland. AAPG Bulletin **73**(9), 1065–1088.

Sneider, J.S., deClarens, P. & Vail, P.R. 1995: Sequence stratigraphy of the Middle to Upper Jurassic, Viking Graben, North Sea. In: Steel, R.J. *et al*. (eds): Sequence stratigraphy on the Northwest European margin. Norwegian Petroleum Society (NPF) Special Publication **5**, 167–197.

Strogen, D.P., Burwood, R. & Whitham, A.G. 2005: Sedimentology and geochemistry of Late Jurassic organic-rich shelfal mudstones from East Greenland: regional and stratigraphic variations in source rock quality. In: Doré, A.G & Vining, B.A. (eds): Petroleum Geology: North-West Europe and Global Perspectives – Proceedings of the 6th Petroleum Geology Conference, 903–912. Geological Society, London.

Surlyk, F. 1973: The Jurassic–Cretaceous boundary in Jameson Land, East Greenland. In: Casey, R. & Rawson, P.F. (eds): The Boreal Lower Cretaceous. Geological Journal Liverpool, Special Issue **5**, 81–100.

Surlyk, F. 1978: Submarine fan sedimentation along fault scarps on tilted fault blocks (Jurassic–Cretaceous boundary, East Greenland). Bulletin Grønlands Geologiske Undersøgelse **128**, 117 pp.

Surlyk, F. 1987: Slope and deep shelf gully sandstones, Upper Jurassic, East Greenland. AAPG Bulletin **71**, 464–475.

Surlyk, F. 2003: The Jurassic of East Greenland: a sedimentary record of thermal subsidence, onset and culmination of rifting. In: Ineson, J. R. & Surlyk, F. (eds): The Jurassic of Denmark and Greenland. Geological Survey of Denmark and Greenland Bulletin **1**, 659–722.

Surlyk, F., Callomon, J.H., Bromley, R.G. & Birkelund, T. 1973: Stratigraphy of the Jurassic–Lower Cretaceous sediments of Jameson Land and Scoresby Land, East Greenland. Bulletin Grønlands Geo-

logiske Undersøgelse **105**, 76 pp. (also Meddelelser om Grønland **193**(5)).

Surlyk, F., Gjelberg, J. & Noe-Nygaard, N. 2007: The Upper Jurassic Hareelv Formation of East Greenland: A giant sedimentary injection complex. In: Hurst, A. & Cartwright, J. (eds): Sand injectites: implications for hydrocarbon exploration and production. AAPG Memoir **87**, 141–149.

Surlyk, F.& Noe-Nygaard, N. 1991: Sand bank and dune facies architecture of a wide intracratonic seaway: Late Jurassic – Early Cretaceous Raukelv Formation, Jameson Land, East Greenland. In: Miall, A.D. & Tyler, N. (eds): The three-dimensional facies architecture of terrigenous clastic sediments, and its implications for hydrocarbon discovery and recovery. SEPM (Society for Sedimentary Geology) Concepts in Sedimentology and Paleontology **3**, 261–276.

Surlyk, F. & Noe-Nygaard, N. 2001: Sand remobilisation and intrusion in the Upper Jurassic Hareelv Formation of East Greenland. In: Surlyk, F. & Håkansson, E. (eds): Oscar Volume. Bulletin of the Geological Society of Denmark **48**, 169–188.

Taylor, G.H., Teichmüller, M., Davis, A., Diessel, C.F.K., Littke, R. & Robert, P. 1998: Organic Petrology, 704 pp. Berlin: Gebruder Borntraeger.

Telnæs, N., Isaksen, G.H. & Douglas, A.G. 1994: A geochemical investigation of samples from the Volgian Bazhenov Formation, Western Siberia, Russia. Organic Geochemistry **21**(5), 545–558.

Vischer, A. 1943: Die postdevonische Tektonik von Ostgrönland zwischen 74° und 75°N. Br. Kuhn Ø, Wollaston Forland, Clavering Ø und angrenzende Gebiete. Meddelelser om Grønland **133**(1), 195 pp.

von der Dick, H., Meloche, J.D., Dwyer, J. & Gunther, P. 1989: Source-rock geochemistry and hydrocarbon generation in the Jeanne d'Arc Basin, Grand Banks, offshore eastern Canada. Journal of Petroleum Geology, **12**, 51–68.

Manuscript received 9 November 2015; revision accepted 10 January 2018